

Characterization of Isotype Heterojunctions
by Capacitance-Voltage
Carrier Concentration Profiling

by

Dubravko Ivan Babic

ECE Report 84-16



DEPARTMENT OF ELECTRICAL AND COMPUTER ENGINEERING
UNIVERSITY OF CALIFORNIA SANTA BARBARA, CALIFORNIA 93106

UNIVERSITY OF CALIFORNIA
Santa Barbara

Characterization of Isotype Heterojunctions by Capacitance-Voltage
Carrier Concentration Profiling

A Dissertation submitted in partial satisfaction
of the requirements for the degree of

Master of Science

in

Electrical and Computer Engineering

by

Dubravko Ivan Babic

Committee in charge:

Professor Herbert Kroemer, Chairman

Professor Stephen I. Long

Professor John G. Skalnik

October 1984

Acknowledgements

Thanks are due to Ernie Caine, Mark Mondry and especially to Bruce Hancock for helpful discussions and growing the samples; to Dr Herbert Kroemer for guidance; and to friends who made my stay at UCSB pleasant.

ABSTRACT

Characterization of Isotype Heterojunctions by Capacitance-voltage Carrier Concentration Profiling

by

Dubravko Ivan Babić

At an isotype heterojunction, the offset in the majority carrier band edge causes the formation of an electric dipole at the interface. The dipole consists of majority carriers, accumulated in a narrow region adjacent to the interface on the notch side of the heterojunction, and of the uncompensated fixed charge of ionized impurities on the depleted side of the barrier. Charge neutrality requires that the sum of accumulated charge, uncompensated charge in the depletion region, and any interface charge, equal zero.

C-V carrier concentration profiling through such a heterojunction from an adjacent Schottky barrier is potentially a good method for determining the band offset ΔE and any interface charge density σ_i . Although the measured apparent carrier concentration profile differs significantly from the true carrier distribution, due to Debye length

averaging, the extraction of ΔE and σ_i from the measured profile by integration is possible, because both the total charge and the first moment of the true carrier distribution are conserved in the profiling process. Using the model for C-V measurement on isotype heterojunctions described by Kroemer and Chien, and the extracted values of ΔE and σ_i , the apparent profile can be reconstructed by computer simulation and compared to the measured one.

The present work concentrates on some topics connected with the determination of the band discontinuity of isotype heterojunctions by C-V carrier concentration profiling:

- i) A method for determining the position of the heterojunction interface from the apparent profile is discussed.
- ii) The abrupt variation of the dielectric permittivity at the interface is incorporated into the interpretation of the C-V data.
- iii) A treatise on profiling through a heterojunction by using a PN-junction rather than a Schottky barrier is given, along with a simple algorithm for the correction of profiles obtained in such a way.

TABLE OF CONTENTS

| | page |
|---|------|
| 1. Introduction | 1 |
| 2. Capacitance methods for determination of the band offset | 3 |
| 2.1 The intercept method | 3 |
| 2.2 C-V carrier concentration profiling | 6 |
| 3. C-V carrier concentration profiling theory | 9 |
| 3.1 Band discontinuity determination | 10 |
| 3.2 Determination of the interface charge density | 13 |
| 3.3 Application to p-type semiconductors | 14 |
| 4. Carrier profile generation | 16 |
| 5. Interface-locating | 18 |
| 6. Effect of dielectric permittivity variation at the interface | 22 |
| 6.1 Profiling through a semiconductor with arbitrary $\epsilon(x)$ | 22 |
| 6.2 Application to isotype heterojunctions | 27 |
| 6.3 Practical application | 31 |
| 7. Heterojunction profiling from a pn-junction | 33 |
| 7.1 The problem | 33 |
| 7.2 The correction algorithm | 37 |
| 8. A problem in experimental band offset determination | 41 |
| 9. Conclusion | 48 |
| 10. Appendix A: The C-V profiling formula | 50 |
| 11. Appendix B: The determination of the band discontinuity using the intercept method | 56 |

| | |
|--|----|
| 12. Appendix C: Simulation of C-V profiling | 62 |
| 13. Appendix D: Computer simulation of C-V profiling | 70 |
| 14. Appendix E: Computer program listing | 80 |
| 15. References | 93 |

1. Introduction

The band offsets appearing at a heterojunction (HJ) interface are essential design parameters for new heterostructure devices. The conduction and the valence band discontinuities, or graded band variations, act as potential barriers for electrons and holes. Carrier confinement or separation, achieved by utilization of this phenomenon, has laid grounds for new devices which outperform conventional homojunction devices. Some of the present applications of HJs are Heterojunction Bipolar Transistors [1,2], High Electron Mobility Transistors [3,4], Heterojunction lasers [5] and Light Emitting Diodes [6].

For practical application of HJs in device design some quantitative predictions of band offsets between two semiconductors are needed. Much theoretical work has been done on this problem. The oldest and still widely used band lineup rule is Anderson's Electron Affinity Rule [7], according to which the conduction band discontinuity should equal the difference in electron affinities of the two semiconductors. A better description of the band lineup is given by the Frenkel-Kroemer Pseudopotential Theory [8]. Currently, the most accurate predictions of band lineups are obtained by Harrison's Linear Combination of Atomic Orbitals theory [9]. Yet, a fully dependable theory has not been developed up to now. Furthermore, the unreliable experimental data make it more difficult to verify the theoretical predictions.

Several experimental techniques have been used for the determination of band discontinuities:

- i) X-ray photoemission spectroscopy (XPS) [10] has been used to measure the valence band discontinuity of some heterojunctions [11].
- ii) The most widely quoted measurement of valence band discontinuity was done by infrared absorption spectroscopy on $(Al,Ga)As / GaAs$ multiple quantum wells, by Dingle [12].
- iii) The current-voltage (I-V) characteristics of pn -heterojunctions may give qualitative information about the band lineup, *if* the lineup is such that the characteristics differ *drastically* from those of homojunctions. If the band lineup is not such an unusual one, the I-V characteristics may also be substantially changed by the presence of any interface charge.
- iv) There are two fundamental capacitance vs. voltage (C-V) techniques [13] for determining the band offsets; the intercept method and C-V carrier concentration profiling method. Both of these methods will be described in the following paragraphs.

2. Capacitance methods for determination of the band offset

2.1. The intercept method

This is a method for determination of the built-in voltage of either homojunctions or heterojunctions. It is basically a measurement of the reverse bias capacitance of a pn -junction as a function of voltage. If both sides of the junction are uniformly doped, then $1/C^2$ is a linear function of the applied voltage (Figure 1), with a slope that is related to the electron and hole concentrations on both sides of the junction [14, Appendix A]. If it were possible to increase the applied voltage into forward bias, one would eventually reach a voltage at which $1/C^2$ intercepts the horizontal axis. In practice this is not possible, because of the interference of the forward bias current and the diffusion capacitance. The point of intercept is therefore found by extrapolating the $1/C^2$ data points from the region of reverse bias, into that of forward bias, as shown on Figure 1. The voltage at which $1/C^2$ becomes zero is called the *intercept voltage*. In the case of a homojunction, the intercept voltage [14,15] equals to

$$V_{int} = V_{bi} - 2 \frac{kT}{q}. \quad (2.1)$$

Here, V_{bi} is the built-in voltage of the pn -junction, given by

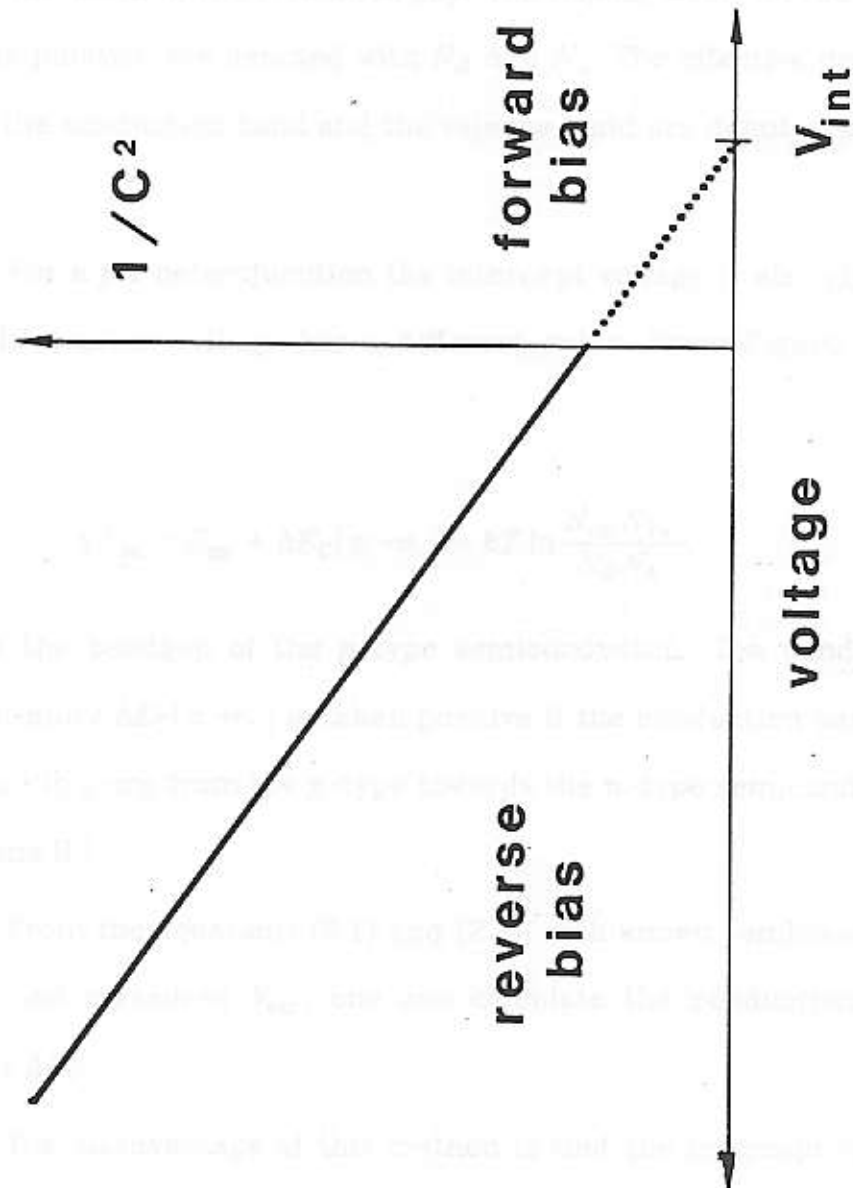


Fig. 1

A plot of $1/C^2$ for a PN-junction with both sides uniformly doped. Extrapolation of data points into forward bias to find the intercept voltage is shown by the dotted line.

$$q V_{bi} = E_g - kT \ln \frac{N_C N_V}{N_D N_A},$$

where E_g is the width of the forbidden gap. The doping levels on the n and p side of the junction are denoted with N_D and N_A . The effective densities of states in the conduction band and the valence band are denoted with N_C and N_V .

For a pn -heterojunction the intercept voltage is also given by (2.1), but the built-in voltage has a different value. From Figure B-1 in Appendix B,

$$q V_{bi} = E_{gp} + \Delta E_C[p \rightarrow n] - kT \ln \frac{N_{Cn} N_{Vp}}{N_D N_A}. \quad (2.2)$$

Here E_{gp} is the bandgap of the p -type semiconductor. The conduction band discontinuity $\Delta E_C[p \rightarrow n]$ is taken positive if the conduction band has a step upward in going from the p -type towards the n -type semiconductor. (See Appendix B).

From the equations (2.1) and (2.2), with known semiconductor parameters and measured V_{int} , one can calculate the conduction band discontinuity ΔE_C .

The disadvantage of this method is that the intercept voltage strongly depends on the presence of any interface charge. The interface charge with surface density σ_i and of any polarity will decrease V_{int} by

$$V_{\sigma} = \frac{q \sigma_i^2}{\epsilon_n N_D + \epsilon_p N_A}$$

(See Appendix B.)

Inasmuch as the result of the measurement is only a single number, namely the intercept voltage, a separate determination of band offset and the interface charge density is not possible. However, the influence of the interface charge on the intercept voltage can be significantly reduced by using very high doping on one side of the HJ. Measurements on such *pn*-heterojunctions have been performed [16].

For an accurate determination of the band discontinuities, one needs to employ a method that is either independent of interface charge or is capable of evaluation of the interface charge density independently from the band offset. The band offset determination using C-V carrier concentration profiling accomplishes this goal.

2.2. C-V carrier concentration profiling

The capacitance method for band offset determination by C-V carrier concentration profiling was first outlined by Kroemer *et al* [17]. It is used exclusively for isotype heterojunctions.

The structure used is shown on Figure 2. A depletion layer is generated outside the HJ, most often by using a Schottky barrier, and its thickness is varied by changing the reverse bias in such a way that the

edge of the depletion passes through the HJ. The C-V data are then used to find the carrier concentration profile* and from there the built-in voltage* and the interface charge density* of the HJ. Measurements of band discontinuities have been performed using this technique [17,18,19,20].

This dissertation is devoted to the problems that occur in application of the C-V carrier concentration profiling method in determining the band offsets of isotype HJs.

* The explanation will be given in section 3.

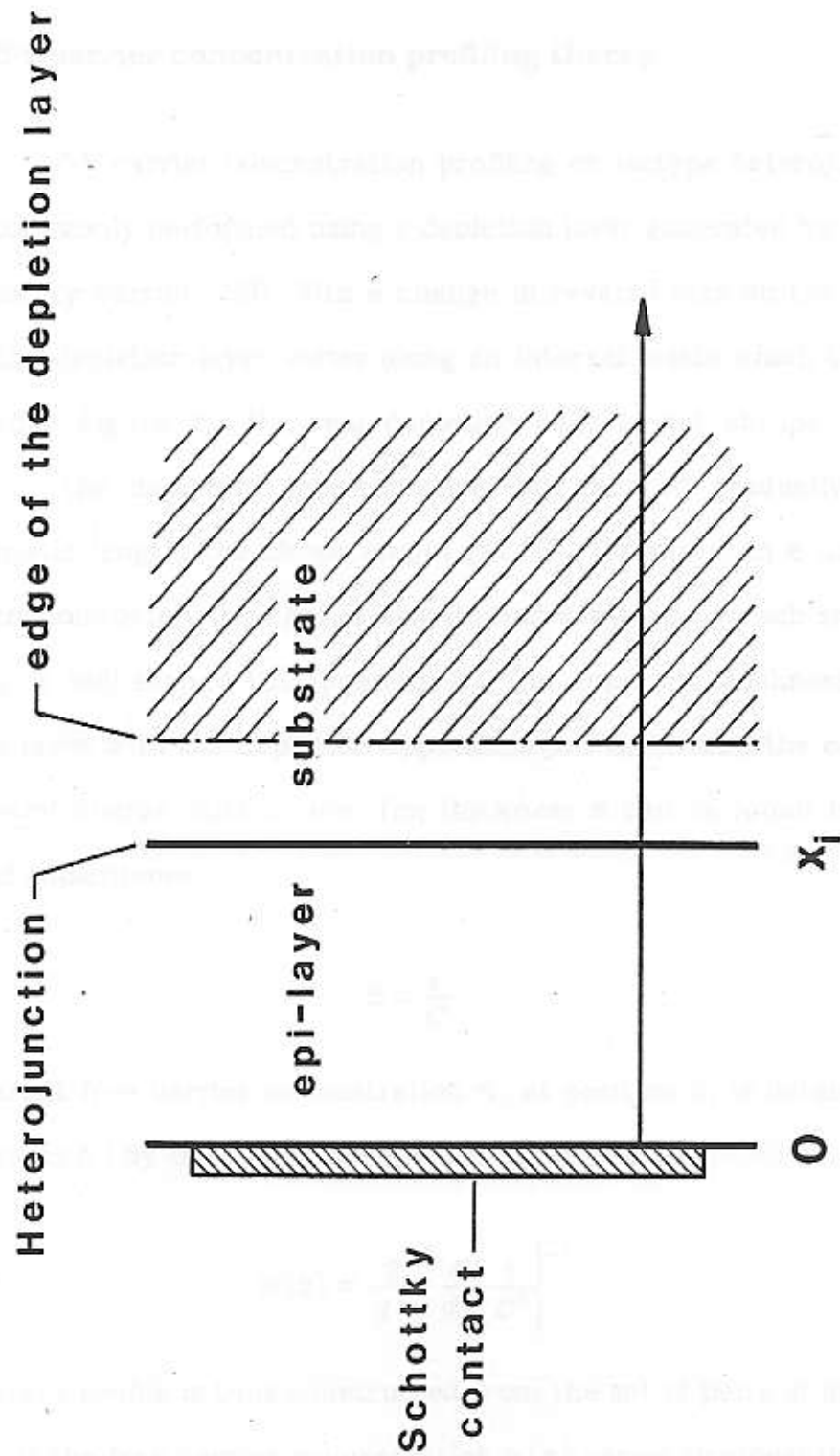


Fig. 2

The structure used for C-V profiling through isotype heterojunctions using a Schottky barrier

3. The C-V carrier concentration profiling theory

C-V carrier concentration profiling on isotype heterojunctions is most commonly performed using a depletion layer generated by an adjacent Schottky barrier (SB). With a change in reverse bias on the SB, the edge of the depletion layer varies along an interval inside which the HJ is located (See Figure 2). The real depletion edge is not abrupt, as it is assumed in the depletion approximation, but falls off gradually with a characteristic length, the *Debye length* [21,22]. Therefore, in a uniformly doped semiconductor, the charge distribution depleted by each small voltage step is bell-shaped [21,Appendix A]. The apparent thickness of the depletion layer \bar{x} in the depletion approximation is, in fact, the center of the depleted charge distribution. The thickness \bar{x} can be found from the measured capacitance:

$$\bar{x} = \frac{\epsilon}{C} \quad (3.1)$$

The apparent free carrier concentration \bar{n} , at position \bar{x} , is determined [See Appendix A] by the conventional C-V profiling formula:

$$\bar{n}(\bar{x}) = \frac{2}{q\epsilon} \left[\frac{d}{dV} \frac{1}{C^2} \right]^{-1} \quad (3.2)$$

The apparent profile is thus constructed from the set of pairs of numbers, \bar{n} and \bar{x} . If the free carrier concentration $n(x)$ varies significantly over a distance of the order of one Debye length, the true $n(x)$ is averaged locally

over few Debye lengths, to form the apparent profile $\bar{n}(x)$ [23]. This effect is especially pronounced in profiling through heterojunctions, because of the large carrier concentration gradients around the interface. In the case of uniformly doped semiconductor [22], $\bar{n}(x)$ equals $n(x)$.

Even though $\bar{n}(x)$ and $n(x)$ may differ significantly, it can be shown that the amount of charge and the built-in electrostatic potential difference of the charge distribution are conserved [21]. This makes possible the extraction of the band offset ΔE of a HJ from the apparent profile, by means of numerical integrations.

3.1. Band discontinuity determination

The structure generally used for profiling through isotype HJ's, consists of two layers: the "substrate" and the "epi-layer", which form a heterojunction at $x = x_i$, as shown in Figure 2. The position variable is taken with respect to the position of the SB. All constants corresponding to the epi-layer, i.e. the layer inside which the depletion is first formed, are here given the subscript 1. The subscript 2 is given to the constants of the substrate.

For the given structure, with a $n-N$ heterojunction and a Schottky barrier, the conduction band discontinuity can be found [17], from

$$\Delta E_C [2 \rightarrow 1] = \frac{q^2}{\epsilon} \int_0^{\infty} [\bar{n}(x) - N(x)] (x - x_i) dx + kT \ln \left[\frac{N_2 N_{C1}}{N_1 N_{C2}} \right]. \quad (3.3)$$

Here $N(x)$ is the doping profile, assumed to be known and to become constant far away from the HJ. N_1 and N_2 are the asymptotic values of the doping levels in the epi-layer and substrate.

If the majority carrier band edge has a step upward when going from the substrate towards the epi-layer, the band offset ΔE_C is counted positive in (3.3). This convention was chosen because it corresponds to a positive conduction band offset for the case currently of greatest interest, an n -type $(Al, Ga)As$ epi-layer on a $GaAs$ substrate.

Using a computer program that simulates C-V profiling on isotype heterostructures, the effect of ΔE variation on the apparent profile is observed. Figure 3 clearly illustrates that a change in the first moment of the charge distribution takes place when the band offset is varied.



Fig. 3. Apparent profile through an isotype heterostructure with $N_1 = 5.4 \times 10^{17} \text{ cm}^{-3}$ and $N_2 = 10^{16} \text{ cm}^{-3}$. The band offset ΔE_C is varied from 0.1 eV to 0.3 eV. The solid line corresponds to $\Delta E_C = 0.1$ eV and the dashed line to $\Delta E_C = 0.3$ eV. The x-axis is the position relative to the Schottky barrier.

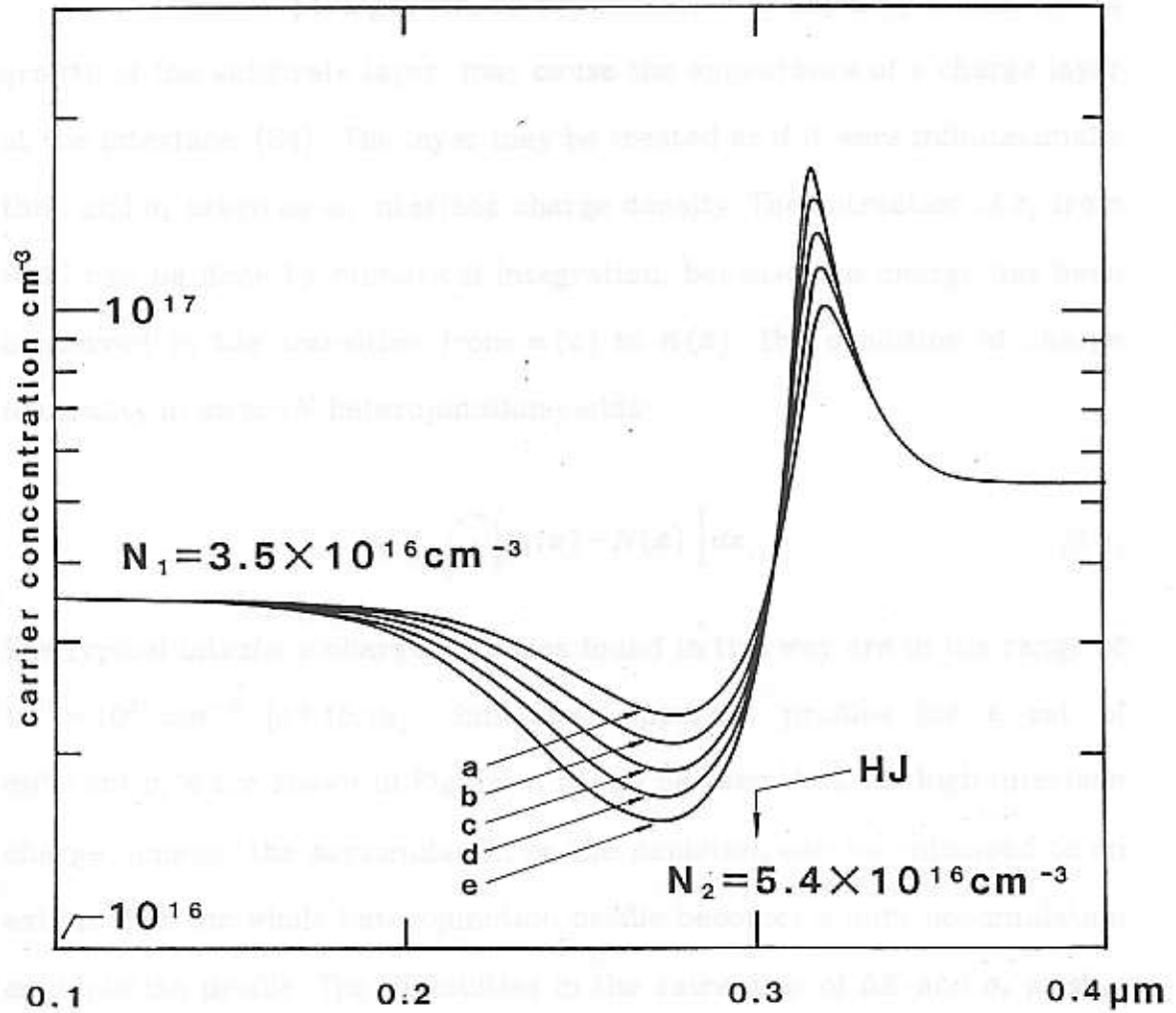


Fig. 3 Apparent profiles through an imaginary heterojunction with $N_1 = 3.5 \times 10^{16} \text{ cm}^{-3}$ and $N_2 = 5.4 \times 10^{16} \text{ cm}^{-3}$. The band offset is the parameter. The values are (a) 100, (b) 120, (c) 140, (d) 160 and (e) 180 meV. The position scale indicates the distance from the Schottky barrier.

3.2. Determination of the interface charge density

Interrupted growth, or accumulation of impurity atoms during growth of the substrate layer, may cause the appearance of a charge layer at the interface [24]. The layer may be treated as if it were infinitesimally thin, and σ_i taken as an interface charge density. The extraction of σ_i from $\bar{n}(\bar{x})$ can be done by numerical integration, because the charge has been conserved in the transition from $n(x)$ to $\bar{n}(\bar{x})$. The condition of charge neutrality in an $n-N$ heterojunction yields

$$\sigma_i = \int_0^{\infty} [\bar{n}(x) - N(x)] dx. \quad (3.4)$$

The typical interface charge densities found in this way are in the range of $10^{10} - 10^{11} \text{ cm}^{-2}$ [17,18,19]. Simulated apparent profiles for a set of different σ_i 's are shown in Figure 4. It can be seen that, for high interface charge density, the accumulation or the depletion can be enhanced to an extent that the whole heterojunction profile becomes a pure accumulation or depletion profile. The difficulties in the extraction of ΔE and σ_i arising from large interface charge, are discussed in Section 5.

3.3. Application to p-type semiconductors

The above formalism, developed for $n-N$ heterojunctions, can be applied to $p-P$ heterojunctions by changing the following variables: The

apparent electron concentration $\pi(x)$ should be replaced by $\bar{p}(x)$, the apparent hole concentration. Similarly, the donor doping profile $N(x)$ should be replaced by $P(x)$, the acceptor doping profile. In the place of the effective density of states in the conduction bands N_{C1}, N_{C2} one should use the effective density of states in the valence bands N_{V1}, N_{V2} , respectively.

When using a p -type material, a positive interface charge density (3.4) represents the density of negative, acceptor-like, interface charge. The rule for the sign of the conduction band discontinuity, given of an n - N heterojunction, holds for the valence band discontinuity ΔE_V , as well.



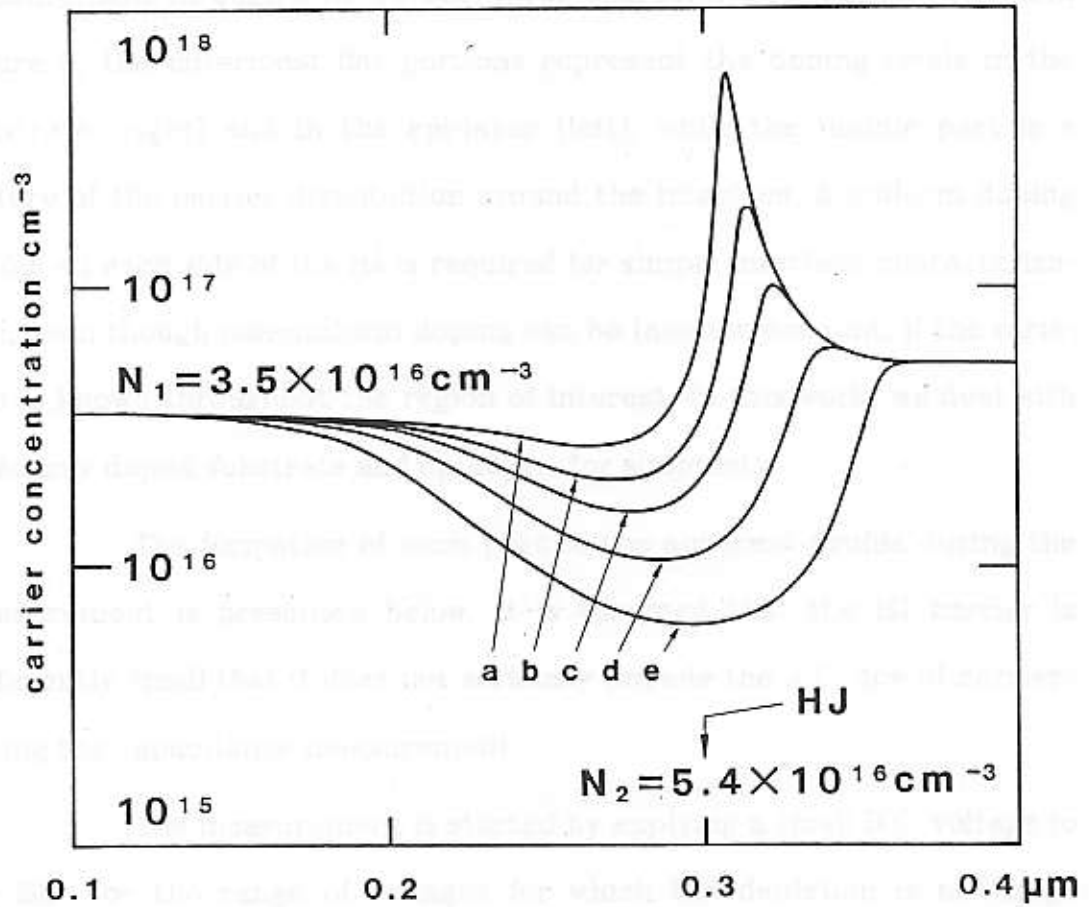


Fig. 4 Apparent profiles through an imaginary heterojunction with $N_1 = 3.5 \times 10^{16} \text{ cm}^{-3}$ and $N_2 = 5.4 \times 10^{16} \text{ cm}^{-3}$. The parameter is interface charge density σ_i . The values are 5, 1, -1, -3 and $-5 \times 10^{11} \text{ cm}^{-2}$, for curves "a" through "e", respectively. The Schottky barrier is placed at $x = 0 \mu\text{m}$.

4. Carrier profile generation

The apparent carrier concentration profile, obtained by C-V measurement through a HJ, reveals three characteristic regions. Shown in Figure 3, the outermost flat portions represent the doping levels in the substrate (right) and in the epi-layer (left), while the middle part is a feature of the carrier distribution around the interface. A uniform doping profile on each side of the HJ is required for simple interface characterization, even though non-uniform doping can be taken in account, if the variation is known throughout the region of interest. In this work, we deal with uniformly doped substrate and epi-layer, for simplicity.

The formation of each part of the apparent profile during the measurement is presented below. It is assumed that the HJ barrier is sufficiently small that it does not seriously impede the A.C. flow of carriers during the capacitance measurement.

The measurement is started by applying a small D.C. voltage to the SB. For the range of voltages for which the depletion is not large enough to affect the HJ carrier distribution, the carriers being depleted come only from the epi-layer, hence the measured $\bar{n}(\bar{x})$ equals the epi-layer doping concentration, N_1 .

By increasing the voltage, the depletion reaches the HJ and induces simultaneous depleting of carriers from the accumulation region and from the edge of the depletion region around the interface. The

apparent carrier profile is being generated by averaging of the true carrier distribution. The resolution depends on the magnitude of the Debye length. The characteristic accumulation and depletion regions around the heterojunction are observed in the apparent profile.

For a sufficiently large bias voltage, most of the carriers being swept away come from the substrate. The HJ is assumed to be all depleted, hence the doping concentration in the substrate is being measured.

The data obtained by measurement can now be used to extract ΔE and σ_i , using (3.3) and (3.4). In order to perform an accurate integration, both doping levels, N_1 and N_2 , have to be known. This means that the measured profile has to flatten out on both sides of the HJ, as shown in Figure 3.

5. Interface-locating

In order to determine the interface charge density σ_i and the band discontinuity ΔE , using (3.3) and (3.4), one needs to know where the heterojunction is located, that is, the value of x_i . The shape of the apparent profile should provide the most relevant data, but unfortunately, there is no feature in the apparent profile that firmly indicates where the interface is located. Note that the true carrier concentration peaks at x_i , whereas the accumulation peak in the apparent profile does not coincide with x_i . An example of a profile from which it would be very hard to locate the interface is shown on Figure 4 with the letter: "e", where a large negative interface charge has repelled all the free carriers around the heterojunction.

One can *estimate* the interface position from the apparent profile by knowing in what region the interface is usually located with respect to the accumulation peak and the depletion valley in the apparent profile. This region can be delimited by using the computer-reconstructed apparent profile of a similar heterojunction, on which the relative position of the interface to the whole apparent profile can be observed. The relationship can now be used to estimate where the interface should be located in the measured profile.

Using the first estimated x_i , the tentative extraction of ΔE and σ_i is performed. What *should have been* the apparent profile is then recon-

structed on a computer, using these obtained data and compared with the measured profile. A further improvement of the x_i estimation may be obtained by comparing the measured and the reconstructed profiles and eventually correcting the initially assumed interface position.

The error introduced by using an inaccurate x_i can be related to the doping levels and the interface charge density. Let x_i^* be the assumed and x_i the true interface position, such that $x_i^* = x_i + \Delta x_i$ (Figure 5) The band offset and the interface charge density obtained by using x_i^* in (3.3) and (3.4), are denoted with σ_i^* and ΔE^* , respectively. From Figure 5 we find that σ_i^* is given by

$$\begin{aligned}\sigma_i^* &= \int_0^{x_i^*} (\bar{n}(x) - N_1) dx + \int_{x_i^*}^{\infty} (\bar{n}(x) - N_2) dx, \\ &= \sigma_i + (N_2 - N_1) \Delta x_i.\end{aligned}\tag{5.1}$$

The band discontinuity ΔE^* is then given by

$$\begin{aligned}\Delta E_C^* &= \frac{q^2}{\epsilon} \int_0^{x_i^*} (\bar{n}(x) - N_1) (x - x_i^*) dx + \\ &+ \frac{q^2}{\epsilon} \int_{x_i^*}^{\infty} (\bar{n}(x) - N_2) (x - x_i^*) dx + kT \ln \frac{N_2 N_{C1}}{N_1 N_{C2}},\end{aligned}$$

which, when integrated, yields

$$\Delta E_C^* = \Delta E_C - \frac{q^2}{\epsilon} \left[(N_2 - N_1) \Delta x_i^2 / 2 + \sigma_i \Delta x_i \right]. \quad (5.2)$$

It can be seen, from the above relations, that a large depletion-forming interface charge, not only reduces the accuracy in determining x_i , but also increases the sensitivity of ΔE to any misplacement of the interface. On the other hand, if the accumulation is enhanced by large σ_i , the determining of the interface position is made even simpler, as seen from the profile "a" in Figure 4.



Fig. 4. Energy band profile with the interface located at x_i . The assumed interface position is marked with x_i .

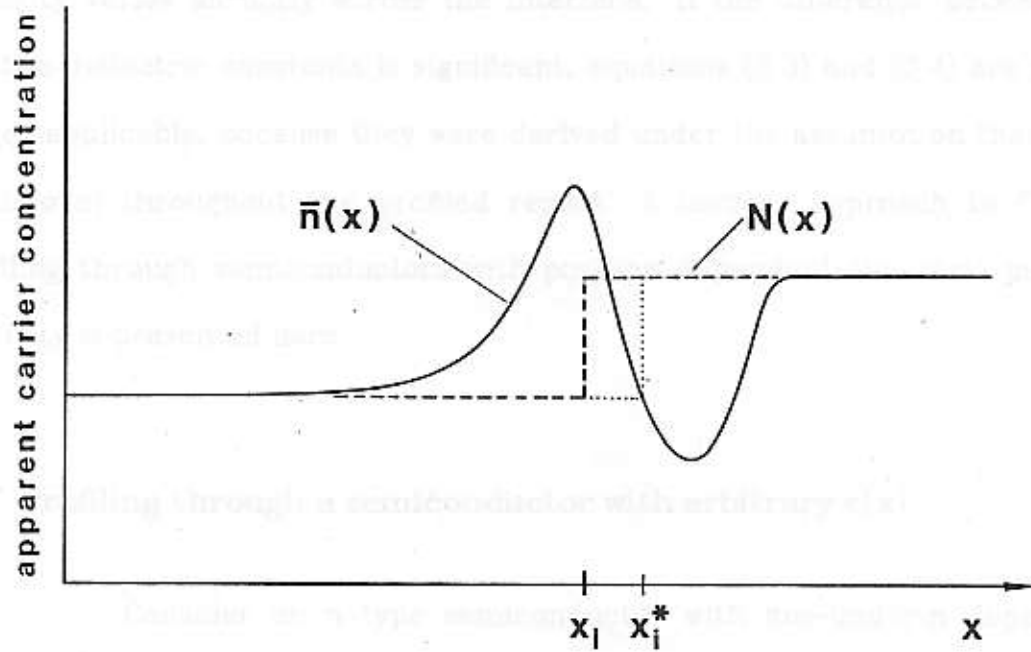


Fig. 5 A heterojunction apparent profile with the true interface position denoted with x_i . The assumed interface position is denoted with x_i^* .

6. Effect of dielectric permittivity variation at the interface

Until now, carrier concentration profiling through a heterostructure has been performed neglecting the fact that the dielectric permittivity varies abruptly across the interface. If the difference between the two dielectric constants is significant, equations (3.3) and (3.4) are no longer applicable, because they were derived under the assumption that ϵ is uniform throughout the profiled region. A correct approach to C-V profiling through semiconductors with position dependent-dielectric permittivity is presented here.

6.1. Profiling through a semiconductor with arbitrary $\epsilon(x)$

Consider an n -type semiconductor with non-uniform doping $N(x)$ and non-uniform dielectric permittivity $\epsilon(x)$. A Schottky barrier is formed at the surface, as shown on Figure 6. The voltage across the depletion layer is sufficiently large, so that all of the carriers near the SB have been depleted, $n(0) = 0$.

A small change in the voltage at the SB will deplete an incremental charge distribution $\Delta n(x)$. The total amount of charge depleted and the magnitude of the voltage increment are given by

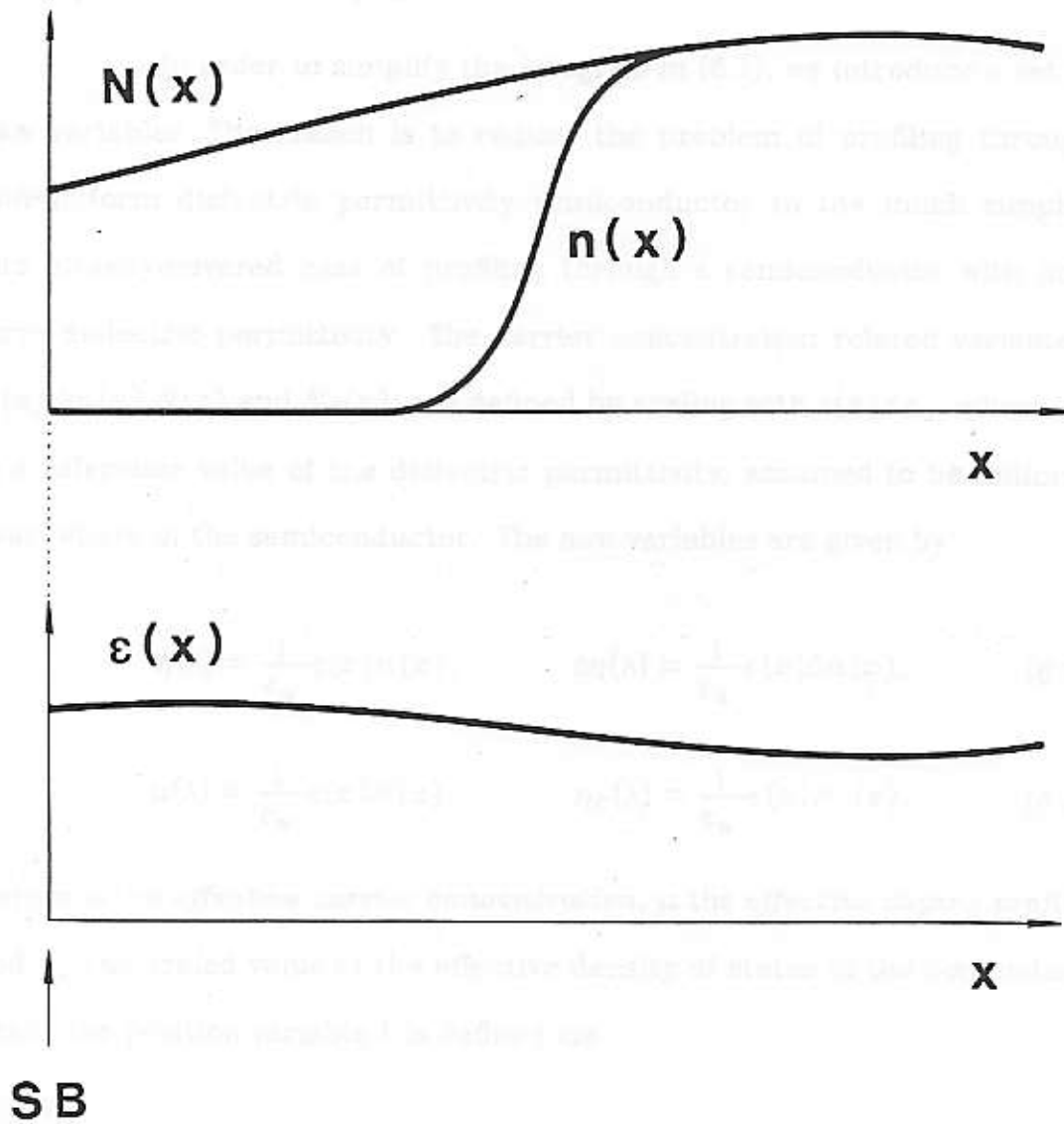


Fig. 6 Non-uniform doping profile and dielectric permittivity of an n -type semiconductor.

$$\Delta Q = q \int_0^{\infty} \Delta n(x) dx \quad \Delta V = q \int_0^{\infty} \frac{dx}{\epsilon(x)} \int_0^x \Delta n(y) dy. \quad (6.1)$$

The capacitance is $C = \Delta Q / \Delta V$.

In order to simplify the integrals in (6.1), we introduce a set of new variables. The reason is to reduce the problem of profiling through non-uniform dielectric permittivity semiconductor to the much simpler and already-covered case of profiling through a semiconductor with uniform dielectric permittivity. The carrier concentration related variables, $n(x), \Delta n(x), N(x)$ and $N_C(x)$, are defined by scaling with $\epsilon(x)/\epsilon_u$, where ϵ_u is a reference value of the dielectric permittivity, assumed to be uniform everywhere in the semiconductor. The new variables are given by

$$\eta(\lambda) = \frac{1}{\epsilon_u} \epsilon(x) n(x), \quad \Delta\eta(\lambda) = \frac{1}{\epsilon_u} \epsilon(x) \Delta n(x), \quad (6.2)$$

$$\mu(\lambda) = \frac{1}{\epsilon_u} \epsilon(x) N(x), \quad \eta_C(\lambda) = \frac{1}{\epsilon_u} \epsilon(x) N_C(x). \quad (6.3)$$

Here η is the *effective carrier concentration*, μ the *effective doping profile* and η_C the scaled value of the effective density of states in the conduction band. The position variable λ is defined via

$$d\lambda = \epsilon_u \frac{dx}{\epsilon(x)} \quad \lambda = \epsilon_u \int_0^x \frac{dy}{\epsilon(y)}. \quad (6.4)$$

It is assumed that the position variation of the dielectric constant is known, so that λ can be expressed as a function of x , therefore all the new

effective variables (6.2), (6.3) can be written as functions of λ .

The amount of charge depleted by a small voltage step and the magnitude of this voltage step are found from the effective carrier distribution by

$$\Delta Q = q \int_0^{\infty} \Delta \eta(\lambda) d\lambda, \quad \Delta V = \frac{q}{\epsilon_u} \int_0^{\infty} \Delta \eta(\lambda) \lambda d\lambda. \quad (6.5)$$

The introduced set of effective variables is sufficient to describe electrostatic phenomena in a semiconductor. The Poisson equation,

$$\frac{d}{dx} \epsilon(x) \frac{dV}{dx} = q (n(x) - N(x)),$$

can, by introducing (6.2), (6.3) and (6.4), be written as:

$$\frac{d^2 V}{d\lambda^2} = \frac{q}{\epsilon_u} (\eta(\lambda) - \mu(\lambda)). \quad (6.6)$$

where $\eta(\lambda)$ is given by:

$$\eta(\lambda) = \eta_c(\lambda) \exp \left(\frac{-qV(\lambda)}{kT} \right). \quad (6.7)$$

The equation (6.6) is in fact the true Poisson equation of a semiconductor with uniform dielectric permittivity equal to ϵ_u , where the doping and the carrier concentration are equal to $\mu(\lambda)$ and $\eta(\lambda)$. The position variable is denoted with λ . Every solution of (6.6) and (6.7) for $\eta(\lambda)$ with a

given voltage as a boundary condition, contains the solution of the Poisson equation in the semiconductor with non-uniform ϵ at the same voltage, because the variable transformations (6.2), (6.3) and (6.4) by definition conserve the total charge and the voltage. The theory, developed for profiling through semiconductors with uniform dielectric permittivity, can now be applied in treating non-uniform permittivity problems by employing the above described variable transformations.

The capacitance, $C = \Delta Q / \Delta V$, is given by

$$\frac{1}{C} = \frac{1}{\epsilon_u} \frac{\int_0^\infty \Delta\eta(\lambda) \lambda d\lambda}{\int_0^\infty \Delta\eta(\lambda) d\lambda} = \frac{\bar{\lambda}}{\epsilon_u}, \quad (6.8)$$

where $\bar{\lambda}$ is the average value of λ from now on referred to as the *apparent effective position* of the depletion edge.

The *apparent effective carrier concentration* is then defined by

$$\bar{\eta}(\bar{\lambda}) = \frac{2}{\epsilon_u} \left\{ \frac{d}{dV} \left(\frac{1}{C^2} \right) \right\}^{-1}, \quad \text{where } \bar{\lambda} = \frac{\epsilon_u}{C}. \quad (6.9)$$

From equations (6.9) it is evident that $\bar{\eta}(\bar{\lambda})$ is what is truly determined in the measurement of the carrier concentration by C-V profiling.

6.2. Application to isotype heterojunctions

Consider an $n-N$ heterojunction with a conduction band diagram shown in Figure 7, and the true carrier distribution and doping profile shown in Figure 8. The epi-layer and the substrate have uniform dielectric permittivities equal to ϵ_1 and ϵ_2 , both sides of the heterojunction are uniformly doped, hence there is an abrupt step in both the dielectric permittivity and the doping profile at the interface. A measured apparent effective carrier concentration profile of such a heterojunction is shown in Figure 9.

Inasmuch as the variable transformations, described in Section 6.1, conserve the total charge and the voltage, the band discontinuity and the interface charge density determined from the equivalent uniform-dielectric-permittivity profile will in fact be true for the non-uniform $\epsilon(x)$ case as well. Therefore, σ_i and ΔE_C are given by

$$\sigma_i = q \int_0^{\infty} (\bar{\eta}(\lambda) - \mu(\lambda)) d\lambda, \quad (6.10)$$

and

$$\Delta E_C = \frac{q^2}{\epsilon_u} \int_0^{\infty} (\bar{\eta}(\lambda) - \mu(\lambda)) (\lambda - \lambda_i) d\lambda + kT \ln \left[\frac{\mu_2 \eta_{C1}}{\mu_1 \eta_{C2}} \right] \quad (6.11)$$

Here λ_i is the position of the interface, $\lambda_i = \lambda(x_i)$. For the case with an abrupt step in the dielectric permittivity at x_i ,

$$\lambda_i = \epsilon_u x_i / \epsilon_1. \quad (6.12)$$

The asymptotic values of the effective doping profile on the two sides of the HJ are denoted μ_1 and μ_2 . The conduction-band-densities of states in the transformed variable system are denoted with η_{C1} and η_{C2} , for the two semiconductors.

With the above presented approach we have the means to evaluate the interface charge density and the band discontinuity taking into account the variation of the dielectric permittivity across the HJ interface.



Fig. 3 The free carrier density (doping) profile of the heterojunction with band diagram shown in Figure 1.

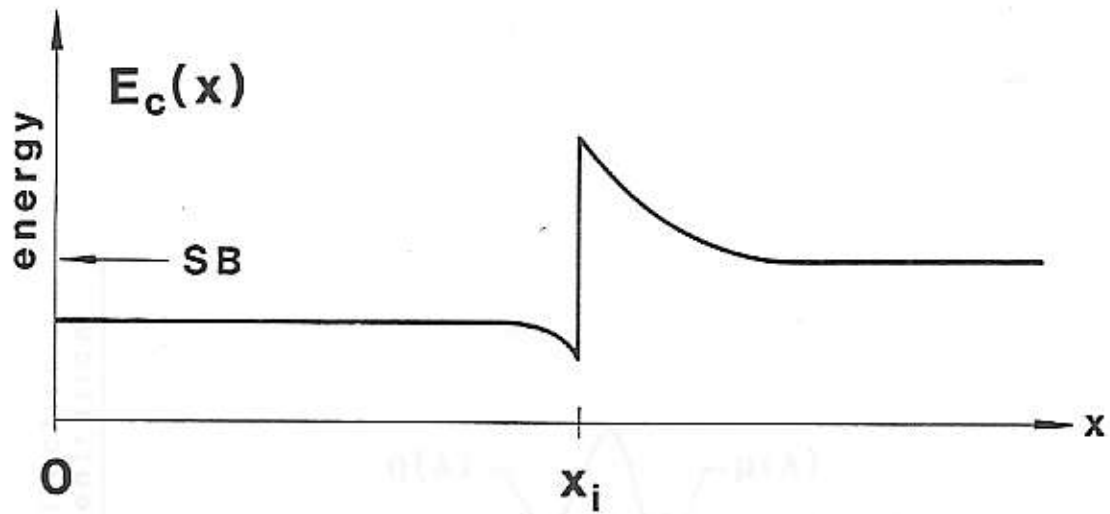


Fig. 7 The conduction band diagram of an n - N heterojunction.

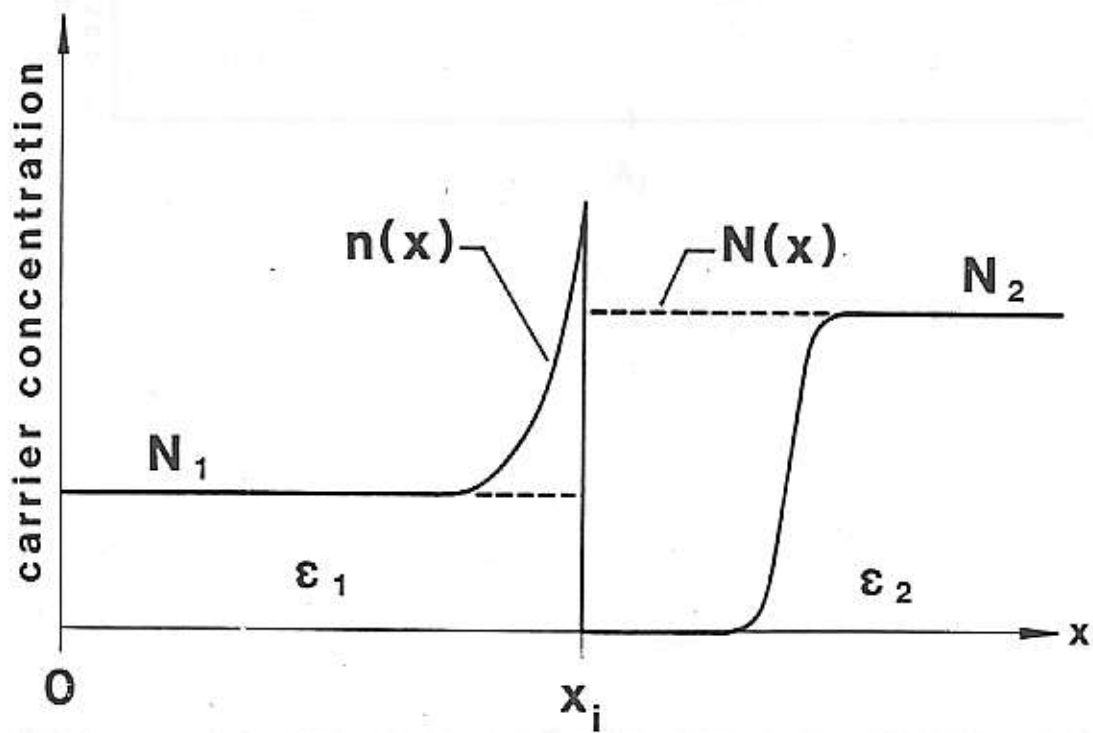


Fig. 8 The free carrier distribution and doping profile of the heterojunction with band diagram shown on Figure 7.

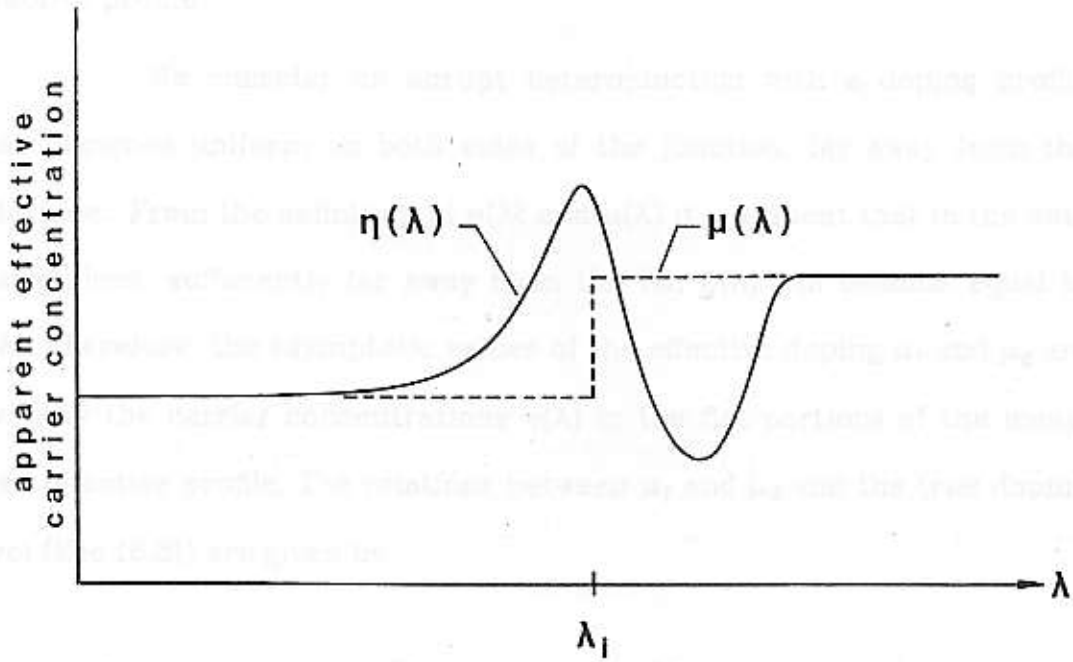


Fig. 9 A typical apparent effective carrier concentration profile through a heterojunction. The position of the interface is denoted with λ_i and the SB is placed at $\lambda = 0$.

6.3. Practical application

To apply the integrals (6.10) and (6.11) in practice we need to make clear how to determine $\mu(\lambda)$ and λ_i from the measured apparent effective profile.

We consider an abrupt heterojunction with a doping profile that becomes uniform on both sides of the junction, far away from the interface. From the definition of $\eta(\lambda)$ and $\mu(\lambda)$ it is evident that in the neutral regions, sufficiently far away from the HJ, $\eta(\lambda)$ will become equal to $\mu(\lambda)$. Therefore, the asymptotic values of the effective doping μ_1 and μ_2 are given by the carrier concentrations $\eta(\lambda)$ in the flat portions of the measured effective profile. The relations between μ_1 and μ_2 and the true doping level (See (6.3)) are given by

$$\mu_1 = \frac{\epsilon_1}{\epsilon_u} N_1 \quad \mu_2 = \frac{\epsilon_2}{\epsilon_u} N_2. \quad (6.13)$$

The dielectric permittivity assumed in the measurement is equal to ϵ_u . The scaling factors $\epsilon_{1,2}/\epsilon_u$ are a result of profiling through a semiconductor with dielectric permittivity different from the one assumed in the calculation of the apparent carrier concentration (6.9). If the true doping levels need to be evaluated from the apparent profile one has to correct the measured value of μ to obtain N by making use of (6.13).

It is important to note that up to now there has not been any constraints on the value of the reference dielectric permittivity ϵ_u . In

profiling through heterojunctions the two immediate choices for ϵ_u are either ϵ_1 or ϵ_2 . There is a significant advantage of setting ϵ_u equal to ϵ_1 , that is, to the dielectric permittivity of the layer closest to the SB: Only in that case λ_i will be equal to x_i (See eq. (6.12)), and the method for determining the interface position, described in Section 5, will yield the actual interface position.

It is evident now that the conventional interpretation of the C-V data has, in fact, been giving accurate results for σ_i and ΔE even in the case when there is an abrupt variation of the dielectric permittivity at the HJ interface. However, the interface position was being determined accurately only when the assumed reference dielectric permittivity was taken equal to ϵ_1 .

7. Heterojunction profiling from a pn-junction

7.1. The problem

Sometimes C-V profiling is done using the depletion layer of a reverse biased pn -junction (See Figure 10) with one side doped much higher than the other. The apparent depletion layer thickness \bar{x}_{pn} , determined from the capacitance, is then a sum of the depletion layer thicknesses [Appendix B] on the n and the p side,

$$\frac{\epsilon}{C} = \bar{x}_{pn} = \bar{x}_n + \bar{x}_p. \quad (7.1)$$

The interpretation of the apparent carrier concentration \bar{n}_{pn} , calculated using (3.2) from the measured C-V relationship, is conceived by differentiating the $1/C^2$ vs. V relation of a pn -junction with respect to voltage. The $1/C^2$ relationship is given with equation (B.11) in Appendix B. The differentiation yields

$$\frac{1}{\bar{n}_{pn}} = \frac{1}{\bar{p}} + \frac{1}{\bar{n}}. \quad (7.2)$$

Here \bar{p} and \bar{n} are the apparent carrier concentrations on the p and n side. It is evident from equations (7.1) and (7.2) that, the apparent position and carrier concentration measured in profiling from a pn -junction, do not correspond the actual apparent profile through a heterojunction and they should not be used to extract the band discontinuity and the interface

charge.

If the doping level of one side of the junction, for example, the p -side, by far exceeds the highest apparent carrier concentration in the n side, $1/\bar{p}$ will be negligible compared to $1/\bar{n}$ in equation (7.2) and the measured carrier concentration \bar{n}_{pn} will then be approximately equal to the apparent carrier concentration \bar{n} on the n side. Due to high doping on the p side, the depletion thickness x_p becomes negligible compared to x_n in equation (7.1). The p^+n -junction generated apparent profile can, therefore, be treated as if it were obtained by profiling from a SB.

The effects of profiling from a pn -junction, with both sides moderately doped, are demonstrated in Figure 11, by means of computer simulation of profiling through an $n-N$ heterojunction. The apparent profile "a" was obtained by profiling using the Schottky barrier and the rest of the profiles, using pn -junctions with various uniform doping levels on the p side. The horizontal position as well as the overall shape of the apparent profile are affected. It is readily visible that the band offset and the interface charge density determined from the profile "d" would not be correct, because the accumulation in "d" has decreased with respect to the one in curve "a", while the depletion has remained almost unchanged. To obtain accurate results, the apparent profile "d" must be corrected.

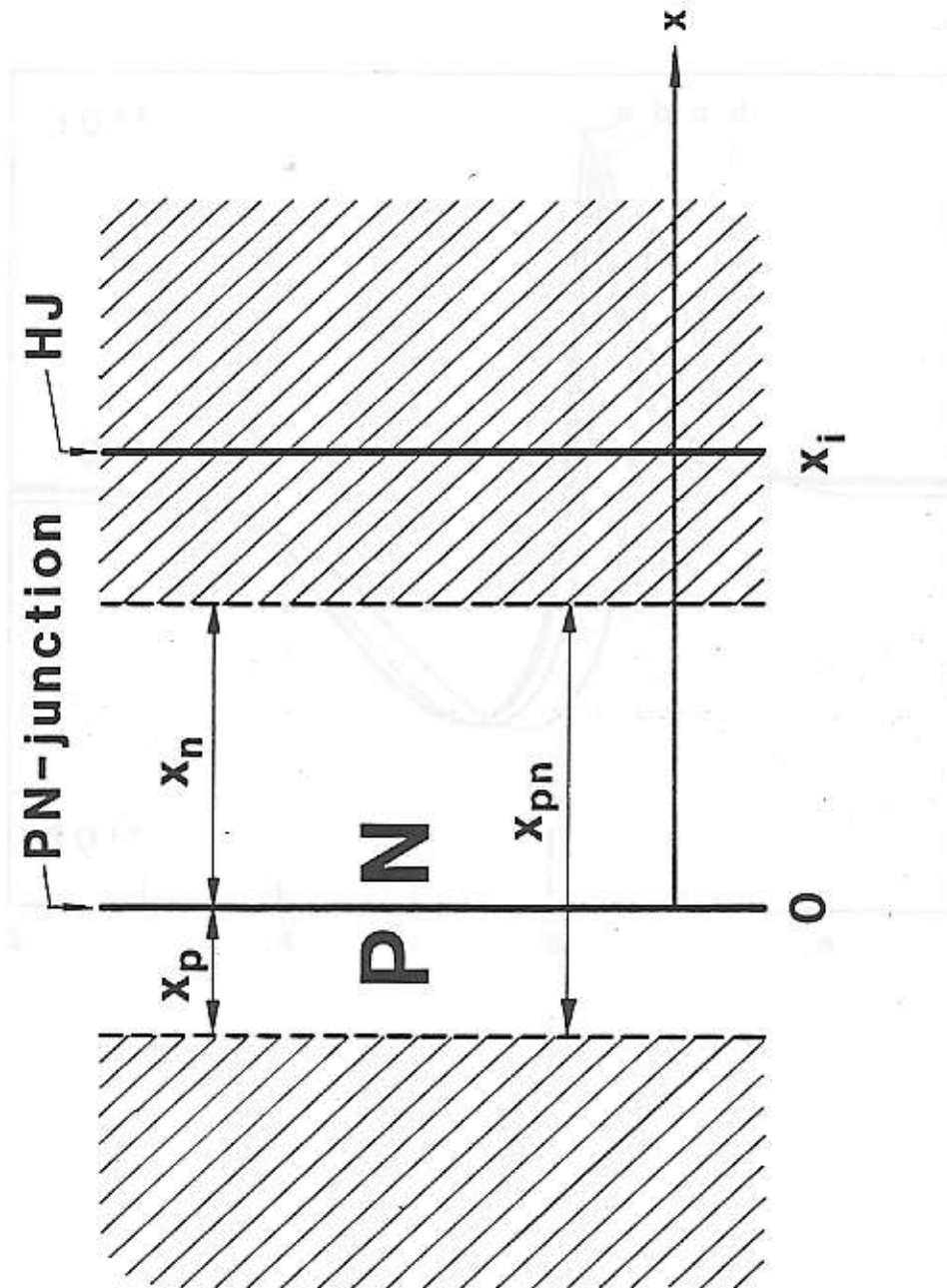


Fig. 10

The structure used for C-V profiling through isotype heterojunctions from a pn -junction.

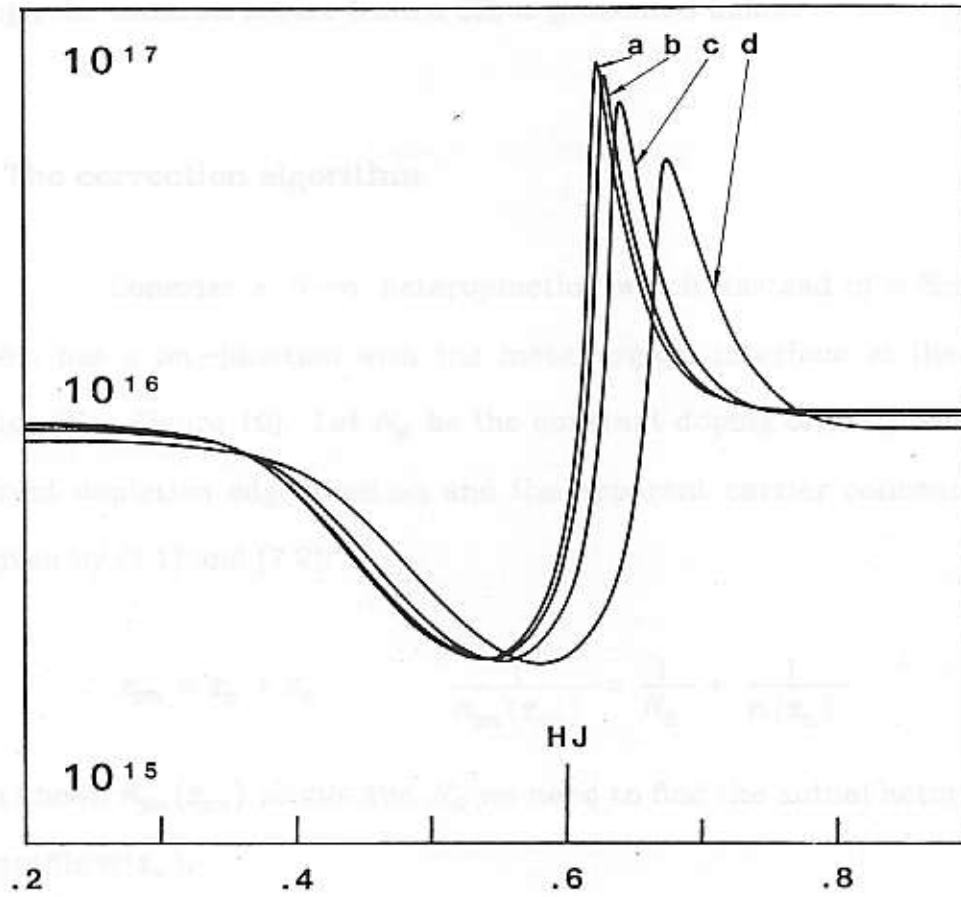


Fig. 11 Simulated apparent profiles through an $N-n$ heterojunction, assuming $\Delta E_C = .33 \text{ eV}$ and $\sigma_i = 0$. (a) Using a Schottky barrier. (b) Using a pn -junction with the p side doped to $N_p = 10^{18} \text{ cm}^{-3}$, (c) $N_p = 3 \cdot 10^{17} \text{ cm}^{-3}$ and (d) $N_p = 10^{17} \text{ cm}^{-3}$.

A simple algorithm that uses an apparent profile obtained by a pn -junction and generates a profile that would be obtained by profiling through the same structure from a SB, is presented below.

7.2. The correction algorithm

Consider a $N-n$ heterojunction which, instead of a Schottky barrier, has a pn -junction with the metallurgical interface at the same position (See Figure 10). Let N_p be the constant doping of the p side. The apparent depletion edge position and the apparent carrier concentration are given by (7.1) and (7.2):

$$\bar{x}_{pn} = \bar{x}_p + \bar{x}_n \quad \frac{1}{\bar{n}_{pn}(\bar{x}_{pn})} = \frac{1}{N_p} + \frac{1}{\bar{n}(\bar{x}_n)}.$$

From known $\bar{n}_{pn}(\bar{x}_{pn})$ profile and N_p we need to find the actual heterojunction profile $\bar{n}(x_n)$.

The apparent position \bar{x}_n on the n side can be determined from the measured \bar{x}_{pn} and \bar{n}_{pn} . Every voltage increment at the pn -junction is going to increase the total depletion thickness \bar{x}_{pn} by $\Delta\bar{x}_{pn}$, where

$$\Delta\bar{x}_{pn} = \Delta\bar{x}_p + \Delta\bar{x}_n. \quad (7.3)$$

The increments in depletion depths on p and n side are denoted with $\Delta\bar{x}_p$

and $\Delta \bar{x}_n$. The amounts of charge depleted from each side of the junction have to be equal, due to charge neutrality.

$$q N_p \Delta \bar{x}_p = q \bar{n}(\bar{x}_n) \Delta \bar{x}_n. \quad (7.4)$$

From (7.2), (7.3) and (7.4) follows an expression for the position increment on the n side as a function of the measured overall thickness increment:

$$\Delta \bar{x}_n = \Delta \bar{x}_{pn} \left(1 - \frac{\bar{n}_{pn}(\bar{x}_{pn})}{N_p} \right). \quad (7.5)$$

The position $\bar{x} = \bar{x}_n$ is found by summing all the increments:

$$\bar{x}_n = \bar{x}_{n0} + \sum \Delta \bar{x}_n. \quad (7.6)$$

The integration constant \bar{x}_{n0} is the apparent depletion depth on the n side at which the profiling was started. The starting position on the measured profile is taken in the neutral part of the epi-layer and denoted with \bar{x}_{pn0} . If it is possible to assume that $\bar{n}_{pn}(\bar{x}_{pn})$ is uniform and equal to N_{pn} in the region between $x + 0$ and \bar{x}_{pn0} ($\approx \bar{x}_{n0}$), then \bar{x}_{n0} can be found by using

$$\bar{x}_{n0} = \bar{x}_{pn0} \left(\frac{N_p - N_{pn}}{N_p} \right). \quad (7.7)$$

This formula was obtained by using (7.1) and (7.2).

If the study of the interface is the objective, any value of \bar{x}_{n0} may be used. The arbitrariness only introduces a shift of the reconstructed profile along the horizontal axis.

In Figure 12 the method is illustrated by means of computer simulation. The profile "a" is obtained by profiling from a Schottky barrier. The apparent profile of the same structure obtained by using a pn -junction which has the p side doped to $N_p = 10^{17} \text{ cm}^{-3}$, is shown by the curve "b". The result of the restoring algorithm is shown by the curve "c". Except for an (intentionally introduced) shift, the two profiles "a" and "c" are almost identical, validating the method presented above. Integration of a restored apparent profile finally gives accurate values for ΔE and σ_i .

The presented method is convenient because the correction of \bar{n}_{pn} and \bar{x}_{pn} can be done at the same time when integration for ΔE and σ_i is performed, since the true doping levels in substrate and epi-layer can be determined in advance by using (7.2) and used in (3.3) and (3.4).



Fig. 12. Apparent profiles through an N - n heterojunction (value as in Figure 11). (a) From a Schottky barrier, (b) From a pn -junction with $N_p = 10^{17} \text{ cm}^{-3}$, (c) Apparent profile "a" as in Fig. 11.

5. A problem in experimental interpretation

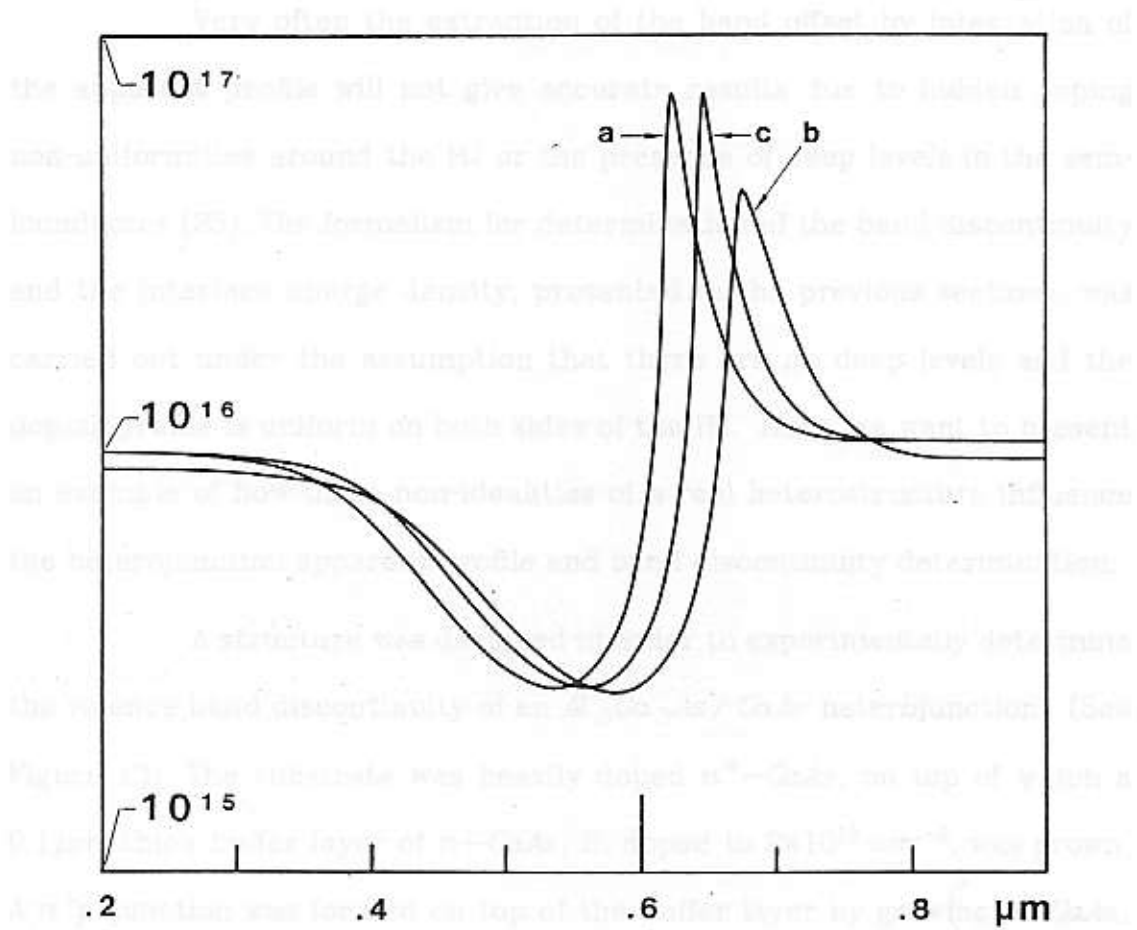


Fig. 12 Apparent profiles through an $N-n$ heterojunction (same as in Figure 11): (a) From a Schottky barrier. (b) From a pn -junction with $N_p \approx 10^{17} \text{ cm}^{-3}$ i.e. profile "d" in FIG. 4. (c) Corrected profile "b".

8. A problem in experimental band offset determination

Very often the extraction of the band offset by integration of the apparent profile will not give accurate results due to hidden doping non-uniformities around the HJ or the presence of deep levels in the semiconductor [25]. The formalism for determination of the band discontinuity and the interface charge density, presented in the previous sections, was carried out under the assumption that there are no deep levels and the doping profile is uniform on both sides of the HJ. Here, we want to present an example of how these non-idealities of a real heterostructure influence the heterojunction apparent profile and band discontinuity determination.

A structure was designed in order to experimentally determine the valence band discontinuity of an $Al_{0.3}Ga_{0.7}As / GaAs$ heterojunction. (See Figure 13). The substrate was heavily doped n^+-GaAs , on top of which a $0.1\mu m$ thick buffer layer of $n-GaAs$, Si doped to $2 \times 10^{18} cm^{-3}$, was grown. A n^+p -junction was formed on top of the buffer layer by growing $p-GaAs$, Be doped to $5 \times 10^{16} cm^{-3}$ and $0.6\mu m$ thick. By growing $0.6\mu m$ of $P-Al_{0.3}Ga_{0.7}As$ doped with Be to $3 \times 10^{16} cm^{-3}$, a $p-P$ heterojunction was formed. A layer of aluminum was deposited "in situ" to form the Schottky contact and etched to form dots needed for capacitance measurements. This structure was intended for profiling through the HJ from two sides, that is, from the SB and from the pn -junction in $GaAs$ below the HJ.

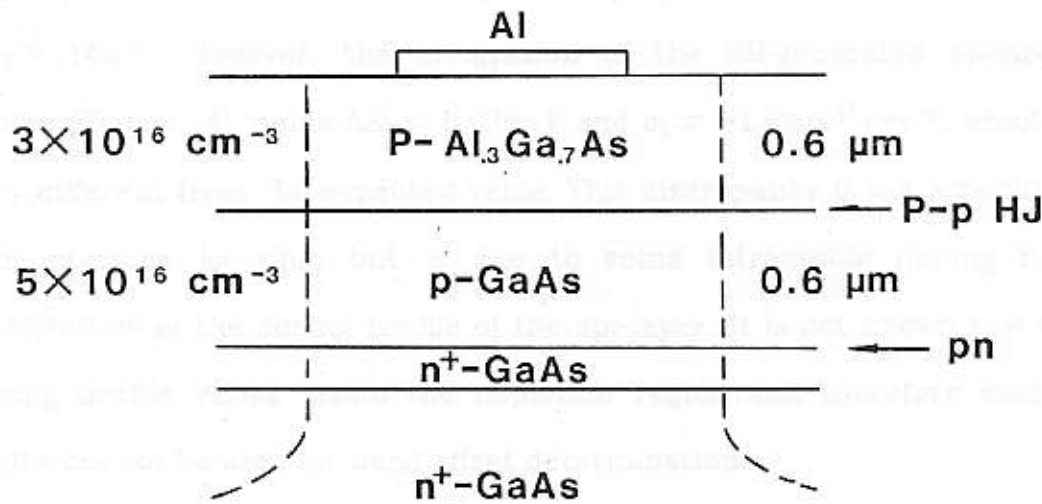


Fig. 13 The structure used for profiling through a p - P GaAs / $Al_{0.3}Ga_{0.7}As$ heterojunction.

First, C-V profiling was performed using the SB and an apparent profile, shown in Figure 14, was obtained. The capacitance of the *GaAs* *pn*-junction was in this measurement assumed to be very large, due to large area (whole wafer $\approx 0.2 \text{ cm}^2$), so that its interference with the SB capacitance measurement could be neglected.

The conduction and the valence band discontinuities of the *Al_{0.3}Ga_{0.7}As* / *GaAs* system are expected [19] to be $\Delta E_C \approx .23 \text{ eV}$ and $\Delta E_V \approx .14 \text{ eV}$. However, the integration of the SB-generated apparent profile (Figure 14) yields $\Delta E_V = 0.078 \text{ eV}$ and $\sigma_i = -1.6 \times 10^{11} \text{ cm}^{-2}$, which is very different from the expected value. This discrepancy is not a result of bad interface locating, but is due to some intractable doping non-uniformities in the doping profile of the epi-layer. It is not known how the doping profile varies inside the depletion region and therefore such a profile cannot be used for band offset determination.

A mesa etch was then performed, shown in Figure 13 with a dashed line, to reduce the reverse saturation current and the area of the *pn*-junction, in order to profile the HJ from the substrate side up i.e. from the *pn*-junction. The measured capacitance is now a series combination of the Schottky barrier and *pn*-junction depletion layer capacitances. Therefore, the apparent profile obtained by profiling from the *pn*-junction will appear to be farther away from the *pn*-junction by a distance equal to the SB depletion layer thickness. The apparent profile shown in Figure 15 is obtained by profiling from the *pn*-junction. The correction for *pn*-

junction-generated profiles, described in Section 7, has not been applied here because the n side of the junction was doped very heavily.

The band discontinuity and the interface charge density determined from the profile shown in Figure 15 are $\Delta E_V = .3 eV$ and $\sigma_i = +2.8 \times 10^{10} \text{ cm}^{-2}$. Inasmuch as both profiles have been obtained by profiling through the same HJ, the measured band offsets and interface charge densities should be approximately equal. The large discrepancy strongly indicates that the structure is not suitable for band discontinuity determination because of some kind of non-uniformity, either in the doping profile or the material composition, the presence of deep levels or some other reasons.

On the pn -junction-generated apparent profile (Figure 15), fitting with a computer reconstructed apparent profile was attempted. A close fit has been obtained with $\Delta E_V = 0.2 eV$ and it is shown by the dotted line in Figure 15. It is visible that, for such a heterojunction, the edge of the depletion and the accumulation peak should be much sharper than they are in the measured apparent profile. The tails with slow falloff, on both sides of the HJ, are the reason why the measured band offset is came out so large.

Any deviation from the ideal conditions, required for band offset determination by C-V carrier concentration profiling method and computer reconstruction, gives rise to anomalous features in the apparent profile making it unsuitable for band discontinuity determination. These

anomalous features can be detected by fitting the measured profile with a computer reconstructed one.

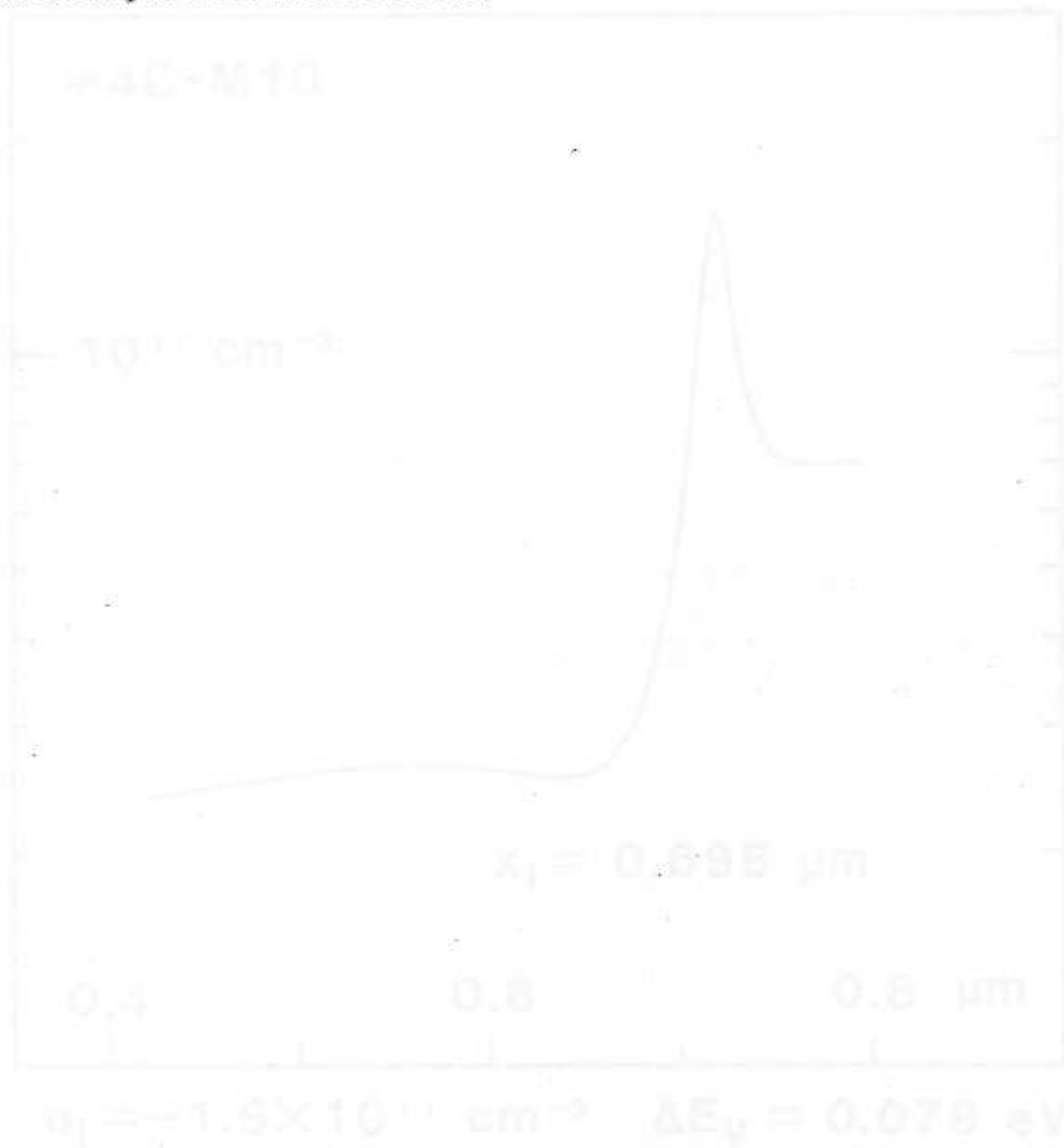


Fig. 12 Experimental profile (dashed line) and computer reconstructed profile (solid line) for sample #4C-M10. The parameters shown in Figure 12, obtained by fitting with the 1D model.

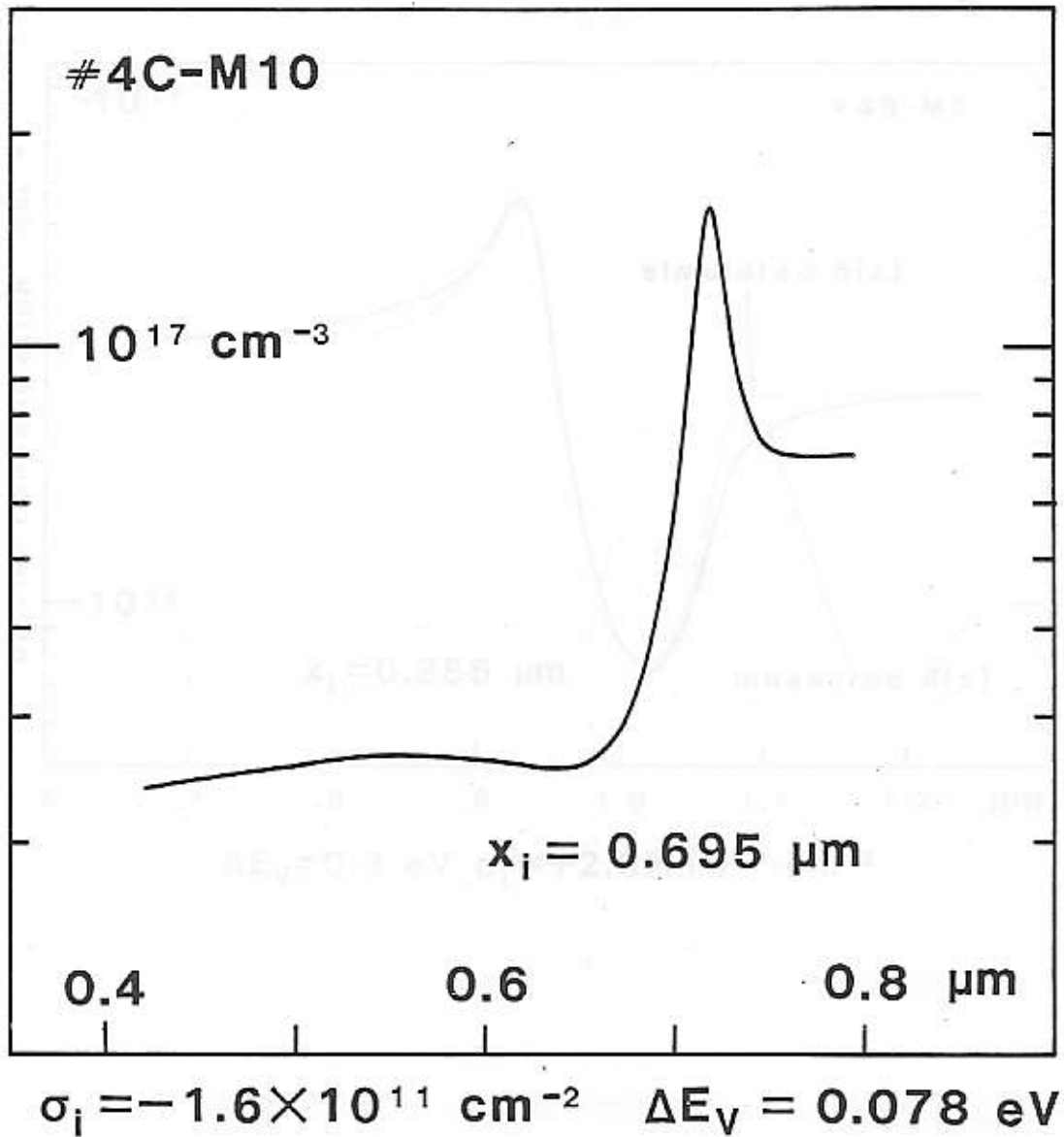


Fig. 14 Experimental apparent profile through the P - p $\text{Al}_{0.3}\text{Ga}_{0.7}\text{As}/\text{GaAs}$ heterojunction shown in Figure 13, obtained by profiling from the SB.

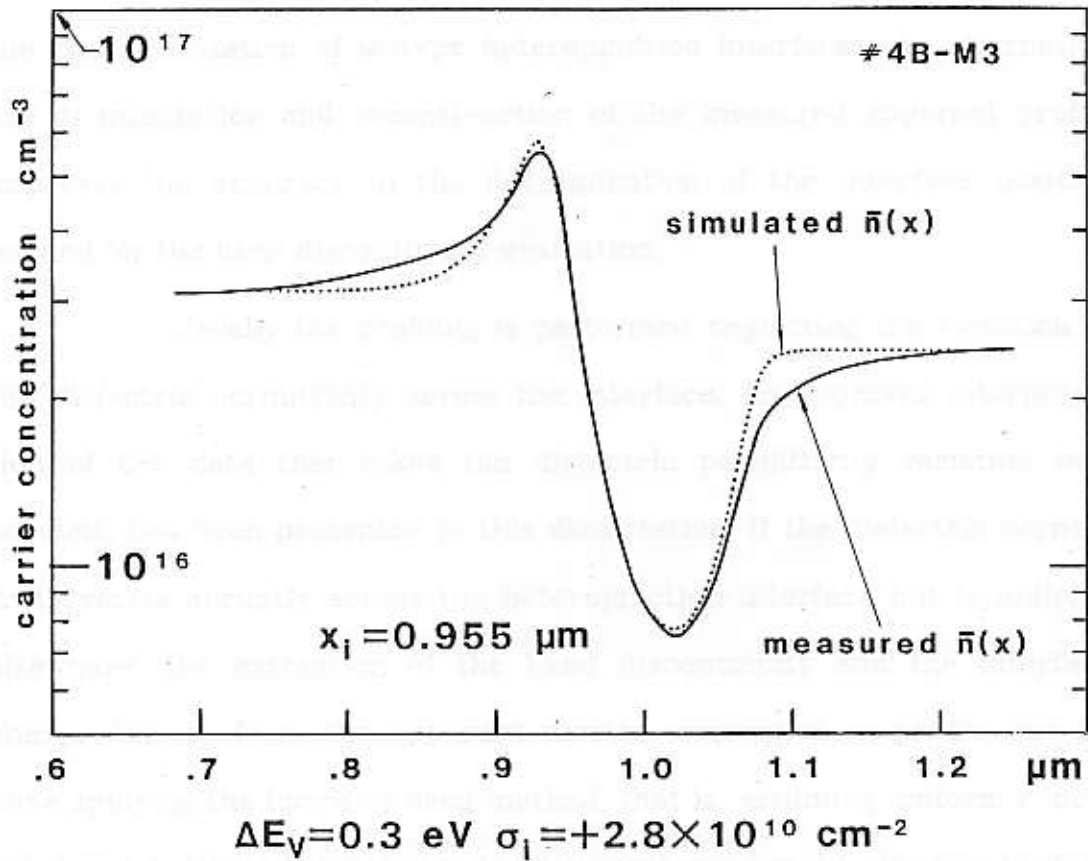


Fig. 15 Experimental apparent profile through the p - P $\text{GaAs}/\text{Al}_{0.3}\text{Ga}_{0.7}\text{As}$ heterojunction shown in Figure 13 (full line), and the attempted fit by computer reconstruction (dotted line).

9. Conclusion

C-V carrier concentration profiling is a promising method for the characterization of isotype heterojunction interfaces. An alternating use of integration and reconstruction of the measured apparent profile improves the accuracy in the determination of the interface position needed for the band discontinuity evaluation.

Usually the profiling is performed neglecting the variation of the dielectric permittivity across the interface. An improved interpretation of C-V data that takes the dielectric permittivity variation into account, has been presented in this dissertation. If the dielectric permittivity varies abruptly across the heterojunction interface but is uniform elsewhere, the extraction of the band discontinuity and the interface charge density from the apparent carrier concentration profile can be done applying the formerly used method, that is, assuming uniform ϵ , provided one distinguishes between the true and measured (effective) values of position, doping levels and carrier concentration.

When a *pn*-junction is used as a depletion generation device, rather than a Schottky barrier, the apparent profile is a result of profiling into both sides of the junction. Inasmuch as only the profile of the side with the heterojunction is of interest, the *pn*-junction apparent profile should be corrected to give a profile that would be obtained if the same structure had been profiled from a SB. Direct integration of the *pn*-junction gen-

erated apparent profile does not give accurate results because of the interference of the charge distribution on the other side of the *pn*-junction. After the profile has been corrected using the simple method explained in Section 7, integration yielding accurate results may be performed.

A reliable experimental heterojunction-band-discontinuity determination by the C-V carrier concentration profiling method is achieved, if the doping profile and the material composition are known throughout the profiled region and if there are no deep levels, that is, the mathematical model of an isotype heterojunction, described in Appendix C, can be applied. Even though the preparation of adequate samples for band offset determination is troublesome, the C-V methods, particularly carrier concentration profiling, serve as an excellent tool in the research of charge phenomena in semiconductors.

10. Appendix A: The C-V profiling formula

C-V profiling from a Schottky barrier is performed using the conventional formula

$$n(x) = \frac{2}{\epsilon q} \left\{ \frac{d}{dV} \left(\frac{1}{C^2} \right) \right\}^{-1}, \quad (\text{A.1})$$

where $n(x)$ is assumed to be the free carrier distribution. Equation (A.1) is true only if the depletion approximation holds, that is if the edge of the depletion is abrupt, as shown on Figure A-1. The capacitance of the structure is given by

$$C = \frac{\epsilon}{x}. \quad (\text{A.2})$$

A voltage increment at the SB will cause the depletion edge to move for Δx , where Δx is assumed to be sufficiently small so that $n(x)$ does not change significantly inside the interval $(x, x + \Delta x)$. The depleted charge distribution is rectangular with height and width equal to $n(x)$ and Δx , respectively. The amount of the depleted charge and the voltage increment can be expressed as

$$\Delta Q = q n(x) \Delta x \quad \Delta V = \frac{q}{\epsilon} n(x) x \Delta x. \quad (\text{A.3})$$

Differentiating $1/C^2$ with respect to the voltage,

$$\frac{\Delta}{\Delta V} \left(\frac{1}{C^2} \right) = \frac{\Delta}{\Delta V} \left(\frac{x}{\epsilon} \right)^2 = \frac{2x}{\epsilon^2} \frac{\Delta x}{\Delta V},$$

and using introducing $\Delta V / \Delta x$ from (A.1), one arrives at

$$\frac{\Delta}{\Delta V} \left(\frac{1}{C^2} \right) = \frac{2}{q\epsilon} \frac{1}{n(x)},$$

which is equivalent to (A.1).

Each voltage step at the SB depletes a number of carriers equal to $\Delta N = \Delta Q / q$, from a region of width equal to Δx , located at x . The measured carrier concentration profile is constructed by plotting the carrier concentration $n(x)$ as a function of the position of the depletion edge x .

The true depletion edge is not abrupt, but falls off gradually with a characteristic length, the *Debye length*, as shown on Figure A-2. A voltage increment at the SB will displace the edge by Δx and the depleted charge distribution $\Delta n(x)$ will be bell-shaped, as shown on Figure A-3. The amount of depleted charge and the voltage increment at the SB can be expressed by

$$\Delta Q = q \int_0^{\infty} \Delta n(x) dx \quad \Delta V = \frac{q}{\epsilon} \int_0^{\infty} \Delta n(x) x dx. \quad (\text{A.4})$$

The depletion layer width, calculated from the capacitance $C = \Delta Q / \Delta V$, is the center of the depleted charge distribution, denoted with \bar{x} :

$$\frac{1}{C} = \frac{1}{\epsilon} \frac{\int_0^{\infty} \Delta n(x) x dx}{\int_0^{\infty} \Delta n(x) dx} = \frac{\bar{x}}{\epsilon}. \quad (\text{A.5})$$

A small voltage step at the SB will deplete a total number of carriers equal to ΔN , with the distribution centered at \bar{x} . The measured carrier distribution is obtained by interpreting the data as if they were obtained with the depletion approximation applicable, that is the, bell-shaped charge distribution shown on Figure A-3 is replaced by a rectangular one which has the same total amount of charge, i.e. ΔN . The carrier concentration profile is then constructed from rectangles having the area and width equal to ΔN and Δx , respectively, placed at \bar{x} . The height of each rectangle is denoted with \bar{n} , where

$$\bar{n}(\bar{x}) = \frac{\Delta N}{\Delta x}. \quad (\text{A.6})$$

The constructed carrier distribution does not show the true free carrier profile, but a profile that was obtained by a process of averaging, while the total charge and the first moment of the charge distribution have been conserved in the transition from $n(x)$ to $\bar{n}(\bar{x})$ [21]. The averaged profile $\bar{n}(\bar{x})$ is referred to as the *apparent profile*. The *apparent carrier concentration* is then given by

$$\bar{n}(\bar{x}) = \frac{2}{\epsilon q} \frac{1}{\frac{d}{dV} \left(\frac{1}{C^2} \right)}. \quad (\text{A.7})$$

where

$$\bar{x} = \frac{\epsilon}{C}. \quad (\text{A.8})$$



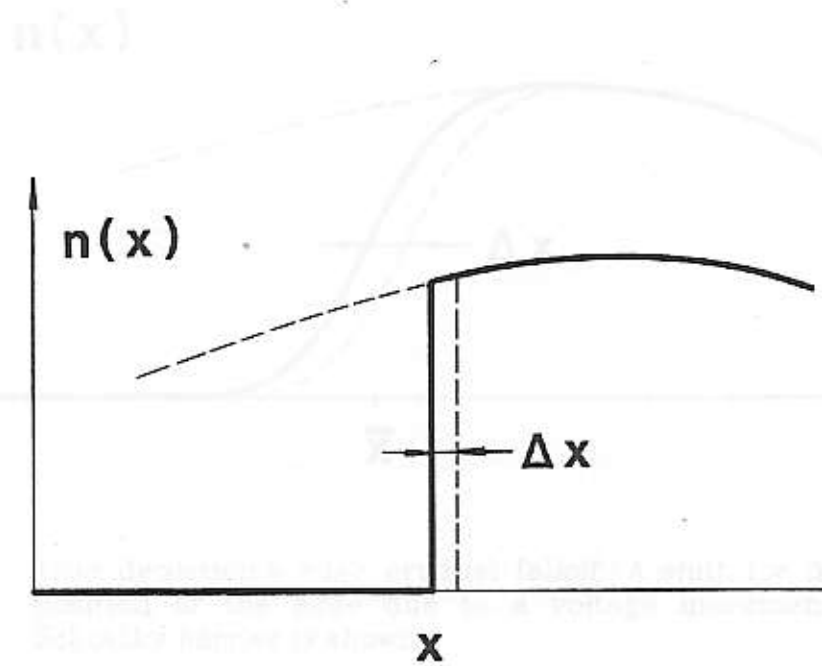


Fig. A-1 The abrupt edge of a depletion layer as it is assumed in the depletion approximation.

11. Appendix B: The determination of the band discontinuity using the intercept method

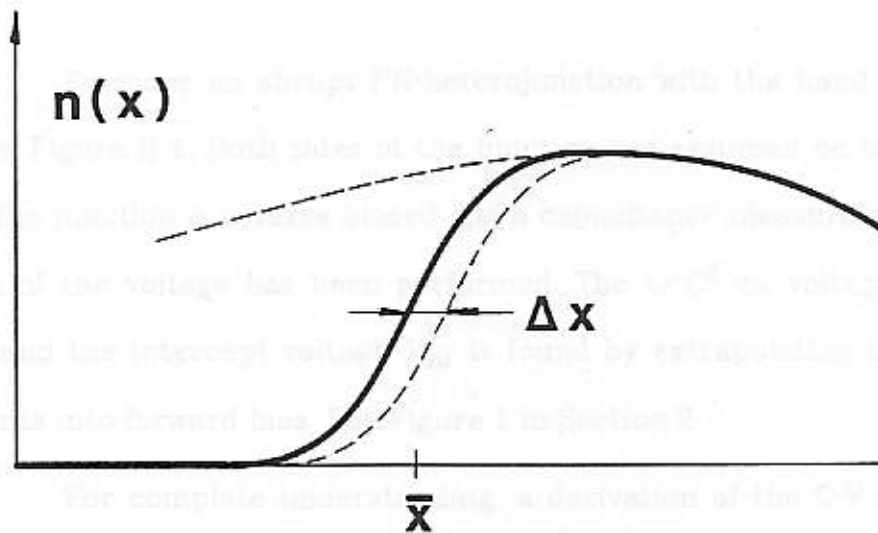


Fig. A-2 True depletion's edge gradual falloff. A shift for Δx in the position of the edge due to a voltage increment at the Schottky barrier is shown.

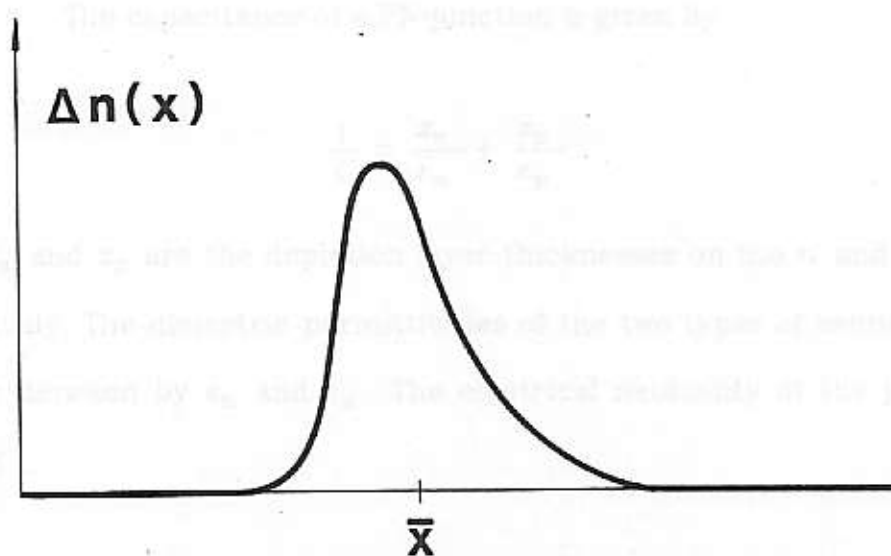


Fig. A-3 The shape of the carrier distribution being depleted by a small voltage step at SB.

11. Appendix B: The determination of the band discontinuity using the intercept method

Consider an abrupt PN-heterojunction with the band diagram shown on Figure B-1. Both sides of the junction are assumed be uniformly doped. The junction is reverse biased and a capacitance measurement as a function of the voltage has been performed. The $1/C^2$ vs. voltage plot is formed and the intercept voltage V_{int} is found by extrapolating the $1/C^2$ data points into forward bias. See Figure 1 in Section 2.

For complete understanding, a derivation of the C-V relationship of a PN-heterojunction is needed. The presence of a charge layer at the interface is incorporated into the derivation ²⁶ [26], because, as it will be seen later, it strongly affects the intercept voltage.

The capacitance of a PN-junction is given by

$$\frac{1}{C} = \frac{x_n}{\epsilon_n} + \frac{x_p}{\epsilon_p} \quad (B.1)$$

where x_n and x_p are the depletion layer thicknesses on the n and p side, respectively. The dielectric permittivities of the two types of semiconductors are denoted by ϵ_n and ϵ_p . The electrical neutrality of the junction requires

$$N_A x_p - N_D x_n = \sigma_i \quad (B.2)$$

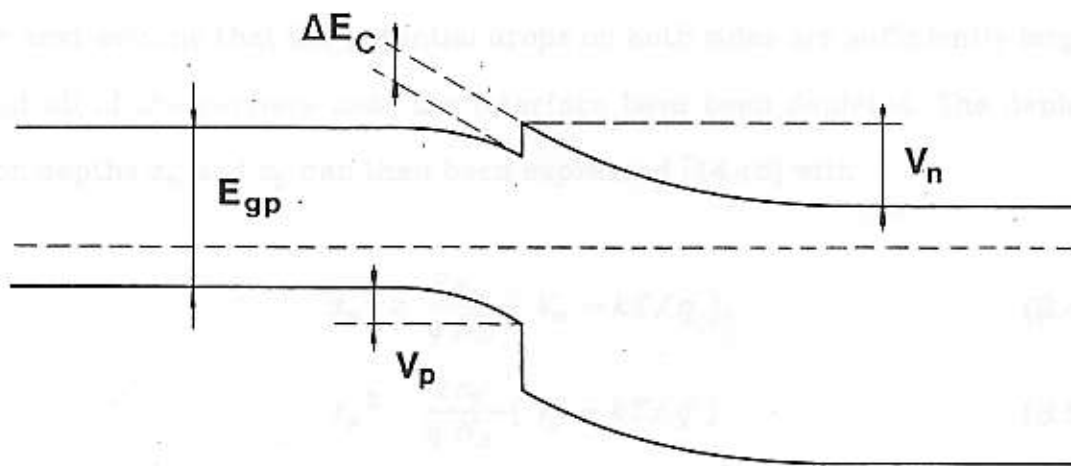


Fig. B-1 A band diagram of a PN-heterojunction with the electrostatic potential drops on the p and n side of the junction denoted with V_p and V_n .

Here, σ_i is the density of interface charges. The doping levels are denoted with N_A for acceptors and N_D for donors. By squaring (B.1) and (B.2) and eliminating the product $x_n x_p$, we arrive at the following equation:

$$\frac{1}{C^2} = \left\{ \frac{N_D x_n^2}{\epsilon_n} + \frac{N_A x_p^2}{\epsilon_p} \right\} \left\{ \frac{1}{\epsilon_n N_D} + \frac{1}{\epsilon_p N_A} \right\} - \frac{\sigma_i^2}{\epsilon_n \epsilon_p N_D N_A}. \quad (\text{B.3})$$

We next assume that the potential drops on both sides are sufficiently large that all of the carriers near the interface have been depleted. The depletion depths x_n and x_p can then be expressed [14,15] with:

$$x_n^2 = \frac{2\epsilon_n}{q N_D} (V_n - kT/q), \quad (\text{B.4})$$

$$x_p^2 = \frac{2\epsilon_p}{q N_A} (V_p - kT/q). \quad (\text{B.5})$$

Here, V_p and V_n are the potential drops across each depletion layer, both taken positive.

Inserting (B.4) and (B.5) into (B.3) one obtains

$$\frac{1}{C^2} = \frac{2}{q} \left\{ \frac{1}{\epsilon_n N_D} + \frac{1}{\epsilon_p N_A} \right\} (V_n + V_p - 2kT/q - V_\sigma), \quad (\text{B.6})$$

where V_σ is a voltage shift due to the presence of the interface charge,

$$V_\sigma = q \frac{\sigma_i^2}{\epsilon_n N_D + \epsilon_p N_A}. \quad (\text{B.7})$$

The sum $V_n + V_p$ consists of: the built-in voltage V_{bi} and any externally

applied reverse bias voltage V . The reverse bias voltage is here counted as positive. The built-in voltage is defined as the value of $V_n + V_p$ in the absence of any external bias.

From the energy band diagram in Figure B-1 one can find that the built-in voltage of an abrupt PN-heterojunction is given by

$$q V_{bi} = E_{gp} + \Delta E_C [p \rightarrow n] - kT \ln \frac{N_{Cn} N_{Vp}}{N_D N_A}. \quad (B.8)$$

Here, E_{gp} is the energy gap on the p-side, and $\Delta E_C [p \rightarrow n]$, the conduction band discontinuity counted positive if the step is upward when going from the p-side to the n-side.

The C-V relationship can now be written as

$$\frac{1}{C^2} = \frac{2}{q} \left\{ \frac{1}{\epsilon_n N_D} + \frac{1}{\epsilon_p N_A} \right\} (V + V_{int}). \quad (B.9)$$

The intercept voltage is then given by

$$q V_{int} = E_{gp} + \Delta E_C [p \rightarrow n] - kT \ln \frac{N_{Cn} N_{Vp}}{N_D N_A} - q V_\sigma - 2kT. \quad (B.10)$$

With known material parameters and no interface charge, equation (B.10) allows the evaluation of the band discontinuity.

It can be seen that the presence of any interface charge of either polarity will reduce the intercept voltage, therefore it is not possible, in this way, to determine neither the band offset nor the interface

charge density accurately. However, the influence of the interface charge on the intercept voltage can be significantly reduced, if one side of the PN-junction is very heavily doped, as seen from equation (B.7).

In order to illustrate this, we first estimate the horizontal shift of the $1/C^2$ plot due to some interface charge density σ_i , if $\epsilon_n = \epsilon_p = 13\epsilon_0$ and $N_D = N_A = 10^{16} \text{ cm}^{-3}$. For a typical interface charge density of $1.2 \cdot 10^{11} \text{ cm}^{-2}$, the intercept voltage will reduce by 0.1 volt. This is too large of an uncertainty for the band offset evaluation. Increasing the doping level of one side of the junction to 10^{18} cm^{-3} , the offset shift drops down to 0.002 volts.

Measurements on PN-heterojunctions having such high doping on one side, have been performed [16].

The $1/C^2$ vs. V relationship for a homojunction can be obtained from equation (B.9), by setting the both dielectric permittivities equal to ϵ ,

$$\frac{1}{C_2} = \frac{2}{q\epsilon} \left(\frac{1}{N_D} + \frac{1}{N_A} \right) (V + V_{int}). \quad (\text{B.11})$$

The intercept voltage is derived from (B.10) by requesting that ΔE_C and σ_i equal to zero and both the density of states in the conduction and valence bands correspond to the same material,

$$qV_{int} = E_{gp} - kT \ln \frac{N_C N_V}{N_A N_D} - 2kT. \quad (B.12)$$

The structure used in simulation is shown in Fig. 1. The structure consists of three parts: the substrate, the epilayer and the Schottky contact. (Figure 1) The model is similar to a $2D$ model of a heterojunction. The epilayer is a 100nm thick GaAs layer on a Si substrate. The epilayer is doped with 10^{18}cm^{-3} Si atoms. The substrate is doped with 10^{18}cm^{-3} Si atoms. The Schottky contact is made of Au on the epilayer. The applied voltage V_{app} is applied between the Schottky contact and the substrate. From these, the carrier concentration and the carrier apparent carrier concentration can be found.

$$n = \frac{qF_{ph}}{qF_{ph} + kT} \quad (B.13)$$

$$p = \frac{qF_{ph}}{qF_{ph} + kT} \quad (B.14)$$

The Hall effect model [2] will be developed for an n -type heterojunction with a Schottky contact on both sides. The heterojunction is made of GaAs epilayer on a Si substrate. The epilayer is doped with 10^{18}cm^{-3} Si atoms. The substrate is doped with 10^{18}cm^{-3} Si atoms. The Schottky contact is made of Au on the epilayer. The applied voltage V_{app} is applied between the Schottky contact and the substrate.

We define a quantity called the quasi-Fermi level potential ϕ_F as follows:

$$-q\phi_F(x) = E_C(x) - E_F(x) \quad (B.15)$$

where $E_C(x)$ is the conduction band edge energy deep in the substrate. The position dependent $\phi_F(x)$ is equivalent to the ϕ_F of the conduction band, but $\phi_F(x)$ decreases exponentially with the distance from the Schottky contact.

1. APPENDIX C: Simulation of C-V profiling

The structure used in simulation of C-V profiling through a heterojunction consists of three parts: the substrate, the epi-layer and the Schottky contact. (Figure 2). In order to simulate a C-V relationship of such a structure, one needs to know the variation of electric field F_{SC} at the Schottky contact, with applied voltage φ_{SC} . From them, the capacitance and the carrier apparent carrier concentration can be found:

$$C = \varepsilon \frac{dF_{SC}}{d\varphi_{SC}}, \quad (C.1)$$

$$\bar{x} = \frac{\varepsilon_1}{C}, \quad \bar{n}(\bar{x}) = \frac{2}{q \varepsilon_1} \left[\frac{d}{dV} \frac{1}{C^2} \right]^{-1}. \quad (C.2)$$

The mathematical model [27] will be developed for an $n-N$ heterojunction with uniform doping on both sides. P -type heterojunctions can be treated with the same formalism. The minority carriers are neglected.

We define a quantity called the *quasi-electrostatic potential* $\varphi(x)$ by

$$-q \varphi(x) = E_C(x) - E_C(\infty)$$

where $E_C(\infty)$ is the conduction band edge energy deep in the substrate. The position dependence of $\varphi(x)$ is equivalent to the one of the conduction band, but $\varphi(x)$ becomes equal to zero whenever the free carrier concentra-

tion equals the uniform doping concentration, either in the substrate or the epi-layer (See equation (C.6) below).

The determination of the $F-\varphi$ relationship will be done separately for the substrate and the epi-layer. If the doping of the substrate is uniform, the electric field can be related to the potential at any position inside the substrate [15].

$$F(x) = \text{sign}(\varphi(x)) \sqrt{2} \frac{V_T}{L_D} \left[\exp\left(\frac{\varphi(x)}{V_T}\right) - 1 - \frac{\varphi(x)}{V_T} \right]^{\frac{1}{2}}. \quad (\text{C.3})$$

Here, V_T is the voltage equivalent of temperature, $V_T = kT/q$. The Debye length L_D is given by,

$$L_D^2 = \frac{\epsilon_2 V_T}{q N_2},$$

where N_2 is the doping level in the substrate. The quasi-potential $\varphi(x)$ exhibits a discontinuity equal to $\Delta E/q$ at the HJ interface (Figure 7). The electric field changes abruptly due to the existence of a layer of charge and abrupt variation of the dielectric permittivity at the interface. The interface charge layer is assumed to be infinitesimally thin and have the areal density σ_i . Therefore, the left and the right limit of $\varphi(x)$ and $F(x)$ at x_i are different, they are related to each other by

$$\varphi(x_i-) = \varphi(x_i+) - \frac{\Delta E_c}{q}, \quad (\text{C.4})$$

$$F(x_i-) = \frac{\epsilon_2}{\epsilon_1} F(x_i+) - q \frac{\sigma_i}{\epsilon_1}. \quad (C.5)$$

Here x_i- and x_i+ symbolize the left and the right limit to x_i . The value of φ and F at position x_i- serve as the boundary condition for solving of the Poisson equation in the epi-layer.

The Poisson equation in the epi-layer is given with:

$$\frac{d^2\varphi}{dx^2} = -\frac{q}{\epsilon_2} \left[N_2 - \frac{N_1 N_{C2}}{N_{C1}} \exp\left(\frac{\varphi}{V_T}\right) \right] \quad (C.6)$$

The factor in front of the exponential function takes in account the difference between the effective densities of states in the conduction bands of the two semiconductors. With given boundary conditions at x_i- a numerical solution of (C.6) is necessary. The integration yields the values of the electric field and the potential at the Schottky contact, $F_{SC} = F(0)$ and $\varphi_{SC} = \varphi(0)$. From the set of F_{SC} and φ_{SC} pairs the C-V relation can be obtained (See Figure C-1).

The procedure is the following. Some value is taken for $\varphi(x_i+)$ and the electric field at x_i+ is calculated using (C.3). The initial conditions for integration of the Poisson equation in the epi-layer are established by using (C.4) and (C.5). The Poisson equation (C.6) is then solved numerically giving the potential φ_{SC} and the electric field F_{SC} at the Schottky contact as a result. Increasing of $\varphi(x_i+)$ in small steps and repeating of the numerical process generates a set of F_{SC} and φ_{SC} pairs which in turn give the C-V relation ship using (C.1).

For the purpose of numerical integration, by using a set of equidistant points, a mesh is formed in the epi-layer (Figure C-2). The separation between points is equal to Δx . The potential and carrier distribution are assumed to take values at these discrete point. The electric field between two adjacent mesh points is defined by

$$F(j) = - \frac{\varphi(j+1) - \varphi(j)}{\Delta x} \quad (C.7)$$

The Poisson equation in the epi-layer is now separated into three equations:

$$n(j+1) = \frac{N_1 N_{C2}}{N_{C1}} \exp\left(\frac{\varphi(j+1)}{V_T}\right) \quad (C.8)$$

$$F(j) - F(j+1) = - \frac{q}{\epsilon_1} \left[N_2 - n(j+1) \right] \Delta x \quad (C.9)$$

$$\varphi(j) - \varphi(j+1) = F(j) \Delta x \quad (C.10)$$

Starting from the initial conditions provided by (C.4) and (C.5), the application of equations (C.8), (C.9) and (C.10) in the presented sequence gives the value of the voltage and the electric field at the SB, where $j = 0$.

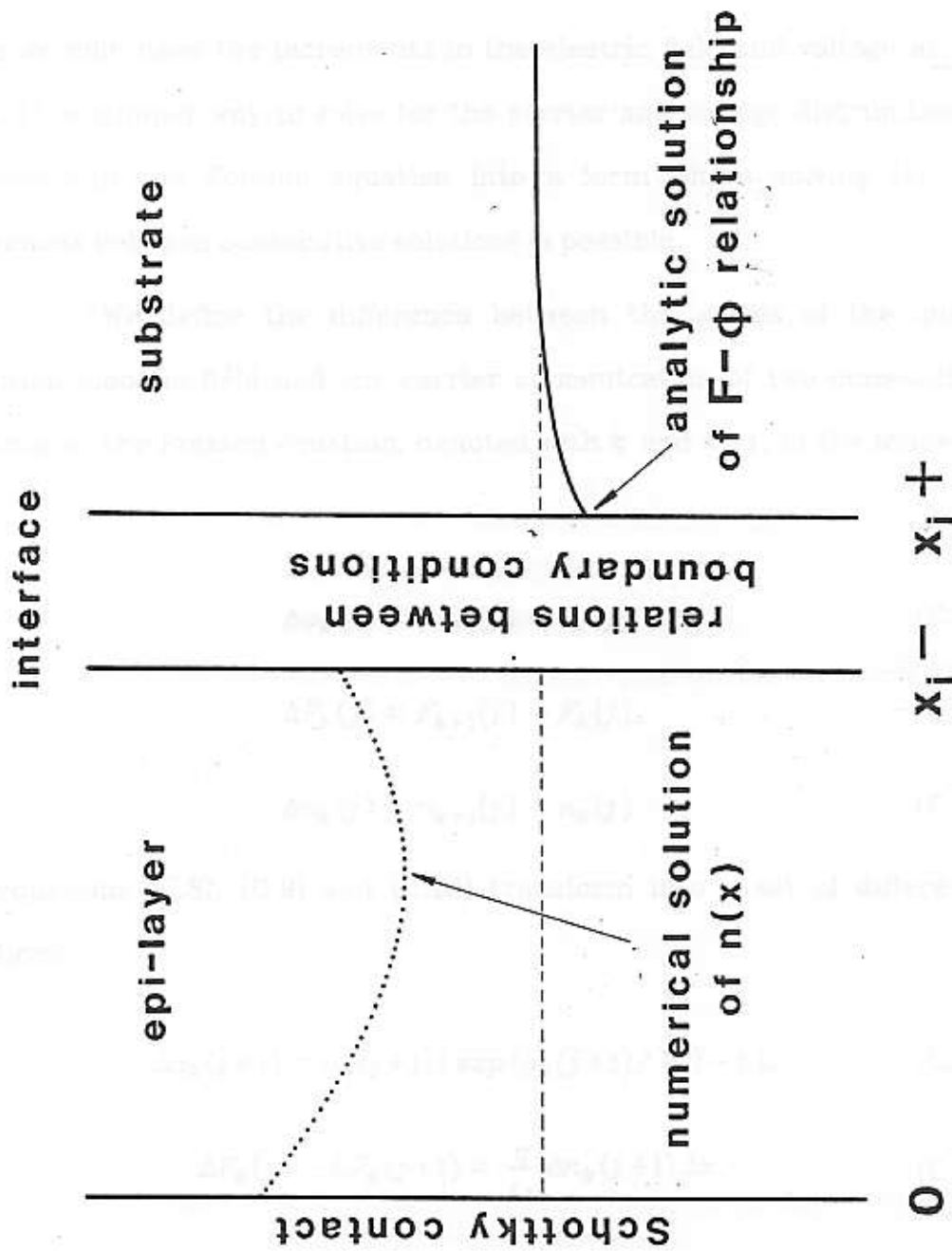


Fig. C-1 Organization of the simulation of the C-V relation of the structure shown on Fig. 2.

Inasmuch as for the position and carrier concentration calculation we only need the increments in the electric field and voltage at the SB (C.1), a simpler way to solve for the carrier and voltage distribution is to transform the Poisson equation into a form where solving for the differences between consecutive solutions is possible.

We define the difference between the values of the quasi-potential, electric field and the carrier concentration of two consecutive solutions of the Poisson equation, denoted with k and $k+1$, in the following way:

$$\Delta\varphi_k(j) = \varphi_{k+1}(j) - \varphi_k(j), \quad (\text{C.11})$$

$$\Delta F_k(j) = F_{k+1}(j) - F_k(j), \quad (\text{C.12})$$

$$\Delta n_k(j) = n_{k+1}(j) - n_k(j). \quad (\text{C.13})$$

The equations (C.8), (C.9) and (C.10) transform into a set of difference equations:

$$\Delta n_k(j+1) = n_k(j+1) [\exp(\varphi_k(j+1)/V_T) - 1], \quad (\text{C.14})$$

$$\Delta F_k(j) - \Delta F_k(j+1) = \frac{q}{\epsilon_1} \Delta n_k(j+1) \Delta x, \quad (\text{C.15})$$

$$\Delta\varphi_k(j) - \Delta\varphi_k(j+1) = \Delta F_k(j) \Delta x. \quad (\text{C.16})$$

The initial conditions for this system can be obtained by applying (C.11) and (C.12) to (C.4) and (C.5). The solution of the above set of equations are

increments in voltage and electric field at the SB. The depletion depth and the apparent carrier concentration are given by,

$$\bar{x}_k = \Delta x \frac{\Delta \varphi_k(0)}{\Delta F_k(0)} \quad (\text{C.17})$$

$$n(x_k) = \frac{\varepsilon_1}{q} \frac{\Delta F_k(0)}{\bar{x}_k - \bar{x}_{k-1}} \quad (\text{C.18})$$

To solve the difference equation system (C.14), (C.15) and (C.16), an initial distribution of carriers $n(j)$ is needed, as it can be seen in (C.14). Therefore, one solution of (C.8), (C.9) and (C.10) is obtained to generate $n(j)$ and then the system (C.14), (C.15) and (C.16) is solved by incrementing $\varphi(x_i +)$. This separates the solving process in two parts: the generation of the initial carrier distribution and generation of the apparent profile by incrementing $\varphi(x_i +)$. The initial $n(j)$ is changed by $\Delta n(j)$ every time a new solution is obtained.

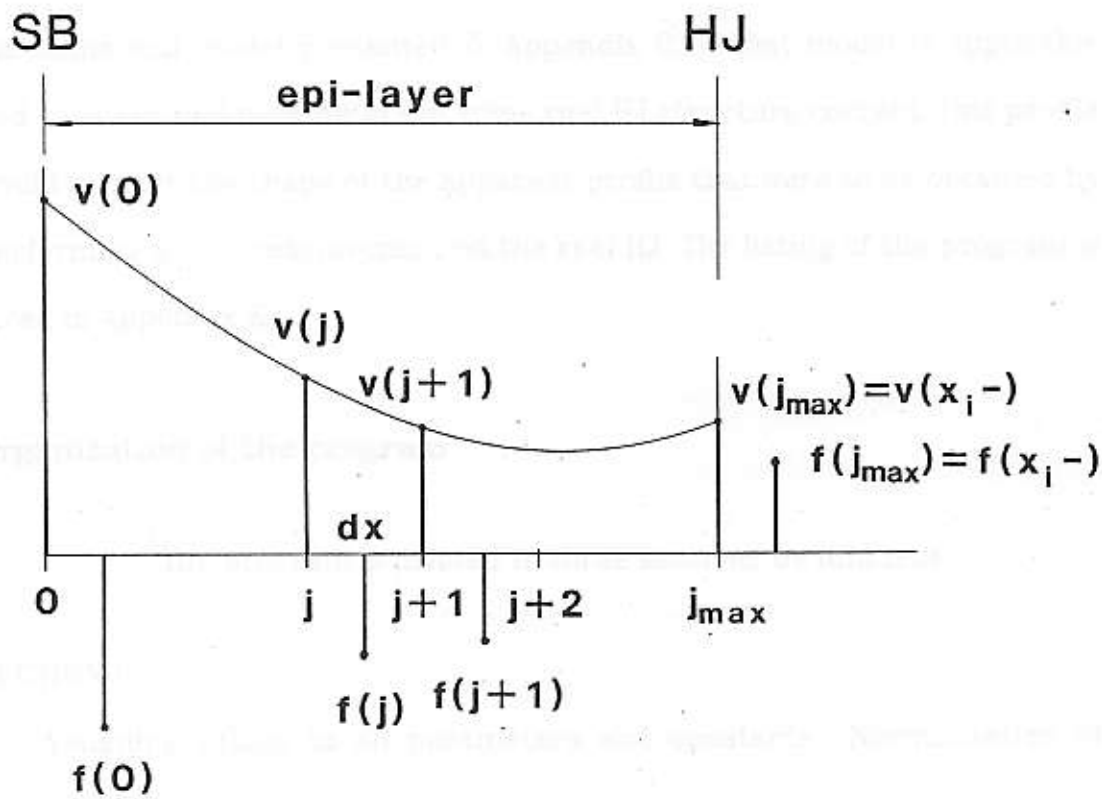


Fig. C-2 The mesh used for numerical solution of the Poisson equation in the epi-layer.

2. Appendix D: Computer simulation of C-V profiling

This appendix describes the organization of a program for simulation of C-V profiling through isotype heterojunctions. The program simulates a measurement of a carrier distribution by means of the mathematical model presented in Appendix C. If that model is applicable and the assumed parameters of some real HJ structure correct, this profile would predict the shape of the apparent profile that were to be obtained by performing a C-V measurement on the real HJ. The listing of the program is given in Appendix E.

Organization of the program

The program is divided in three sections by function.

SECTION I:

Assigning values to all parameters and constants. Normalization of variables.

SECTION II:

Solution of Poisson equation to generate the initial carrier distribution.

SECTION III:

Solution of the Poisson equation in the form of a set of difference equations (C.14), (C.15) and (C.16). Generation of the apparent profile.

Each of these sections is discussed in detail below.

SECTION I

The input data can be divided into four groups:

General (Temperature and semiconductor type),

Heterojunction data (Band offset and interface charge density),

Substrate and Epi-layer data (Doping level, effective density of states and dielectric permittivity).

The default values for all material parameters are assigned the values for GaAs at the beginning the program. (A subroutine named CHANGE allows the user to change all these parameters from the terminal. This subroutine is activated by simply running the program.) The data for GaAs, (AlGa)As, Si and GaP are already stored in the program and are accessible through a subprogram DATA. There is also the possibility of entering data of some other semiconductor through the terminal.

For easier manipulation in the program, all of the variables are normalized. The normalization is shown below.

$$v(j) = -\frac{\varphi(j)}{V_T} \quad (D.1)$$

$$f(j) = \frac{F(j)\Delta x}{V_T} \quad (D.2)$$

$$d(j) = \frac{n(j)(\Delta x)^2 q}{V_T \epsilon_1} \quad (D.3)$$

$$DD = \frac{N_1(\Delta x)^2 q}{V_T \epsilon_1} \quad (D.4)$$

$$A = \frac{N_{C1}}{N_{C2}} \frac{N_2(\Delta x)^2 q}{V_T \epsilon_1} \quad (D.5)$$

SECTION II: Analysis of the initial state

Using the above normalizations the equations (C.8), (C.9) and (C.10) transform into:

$$d(j+1) = A \exp(-v(j+1)) \quad (D.6)$$

$$f(j) - f(j+1) = -(DD - d(j+1)) \quad (D.7)$$

$$v(j) - v(j+1) = -f(j) \quad (D.8)$$

This set of equations is to be solved to obtain the initial carrier distribution in the epi-layer. The solution has to be done with as small band bending as possible. In that case the depletion region at the contact will be small and will not affect the carrier distribution around the HJ interface, that is, a flat portion in the apparent profile will be observed on the epi-layer side. Inasmuch as the only independent variable in the algorithm is $v(x_i+) = -\varphi(x_i+)/V_T$, this quantity is adjusted by bisection until $v(0) = -\varphi_{SC}/V_T$, becomes close to zero. In practice we request that

$$0 < v(0) < 3, \quad (D.9)$$

that is, the voltage at the Schottky barrier is between 0 and $3kT/q$.

To visualize the process, we show in Figure D-1 some examples of Poisson equation extrapolation where the chosen $v(x_i +)$ is too small or too large. We also show the case where the condition (D.9) is met.

The interval length in the mesh Δx and the epi-layer width is adjusted according to the level of doping in the epi-layer with

$$N_1 \times \omega^2 = \text{constant}, \quad \omega = \Delta x \times n. \quad (D.10)$$

Here ω is the distance between the SB and the heterojunction and n is the number of discrete mesh points in the epi-layer. Under the above conditions, the voltage needed to deplete the whole epi-layer will for all epi-layer doping levels remain approximately the same. The constant in (D.10) is adjusted in such a way that for band offsets $\Delta E < 0.7 \text{ eV}$, and interface charge densities $|\sigma_i| < 1 \times 10^{12} \text{ cm}^{-2}$, the distance between the SB and the heterojunction is large enough that the flat portion of the apparent profile in the epi-layer will always be present. The shape of the apparent profile does not depend on how far away the SB is from the HJ, as long it is sufficiently far so it does not interfere with HJ carrier distribution. In Figure D-2 we show two apparent profiles, one with the SB too close and the other one sufficiently far away. The thickness of the epi-layer is set automatically in the program, but sometimes the combined influence of large ΔE and large σ_i will require an increase in the epi-layer thickness.

This happens when the depletion region thickness is of the order of or larger than the epi-layer. Readjustment of ω is possible from the terminal.

In the case where the accumulation notch is on the substrate side and the carrier concentration inside is expected to exceed the effective density of states, the possibility of using the Joyce-Dixon approximation [15,28] is offered in the program. The $F-\phi$ relationship at x_i+ is determined by the subroutine DIXON. A flag is set in section I of the program to indicate whether the approximation should be applied or not. It can only be applied for accumulation appearing on the substrate side of the interface. The approximation works well with carrier concentrations as high as 20 times the effective density of states, but diverges above this value. This divergence sets a limitation on the largest possible value of the band discontinuity and interface charge density that can be used in the simulation. If the carrier concentration in the accumulation notch on the substrate side of a heterojunction with no bias at the SB exceeds $20 \times N_C$, the extrapolation of the Poisson equation will not be possible. In this case the program will exit announcing: "EXECUTION TERMINATED - extrapolation to the surface cannot be done". This message will also appear in every other case where the extrapolation was unsuccessful.

Inasmuch as the program contains no Joyce-Dixon approximation for the accumulation on the epi-layer side, the limit on the magnitude of the band discontinuity and the interface charge density is set by the requirement that the carrier concentration in the accumulation notch

must not exceed the effective density of states.

After the initial carrier distribution and the corresponding $v(x_i+)$ are found, the program proceeds to the difference analysis, Section III.

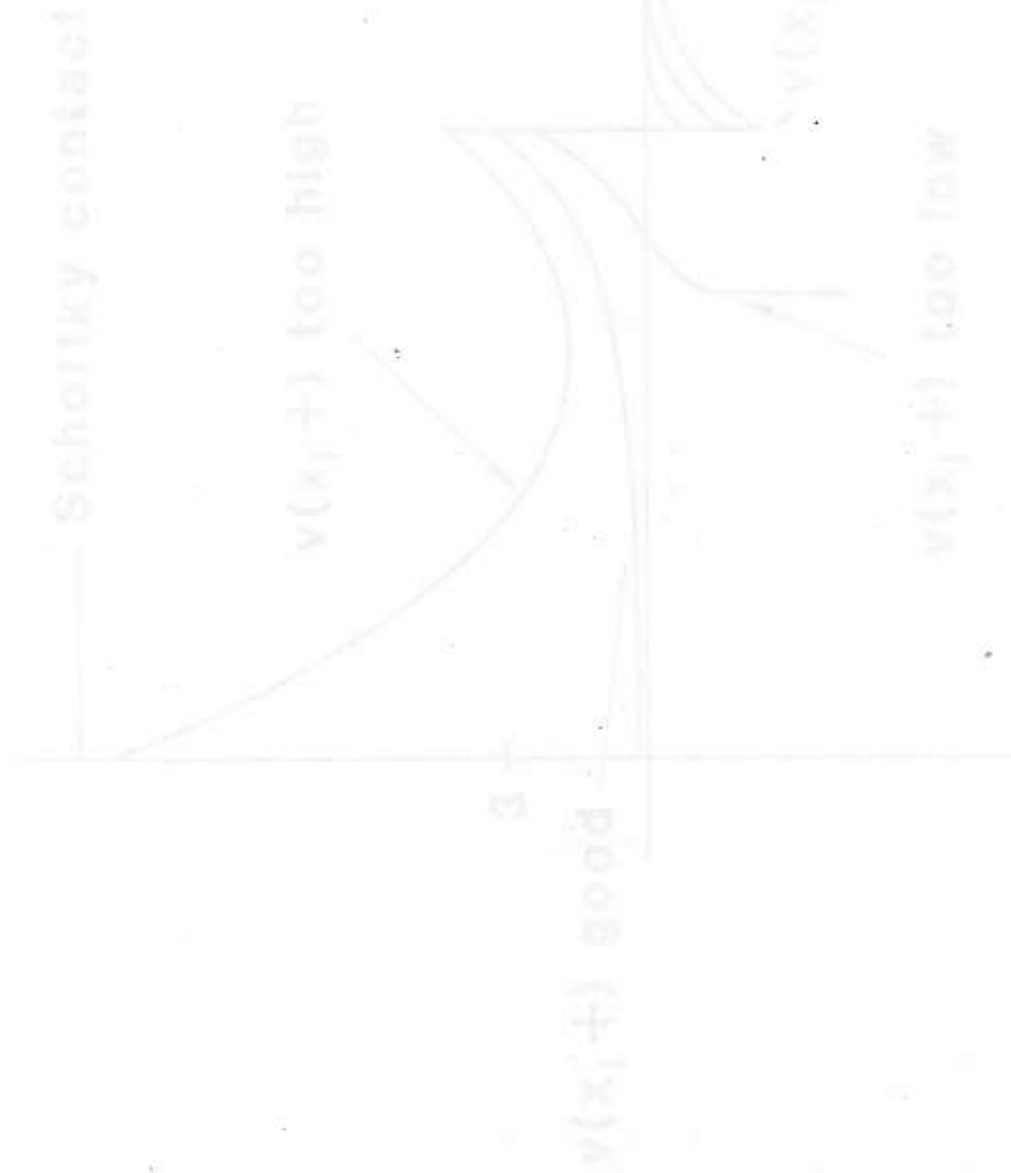


(Fig. D-1)

Effects of bad alignment of the potential $v(x_i+)$.

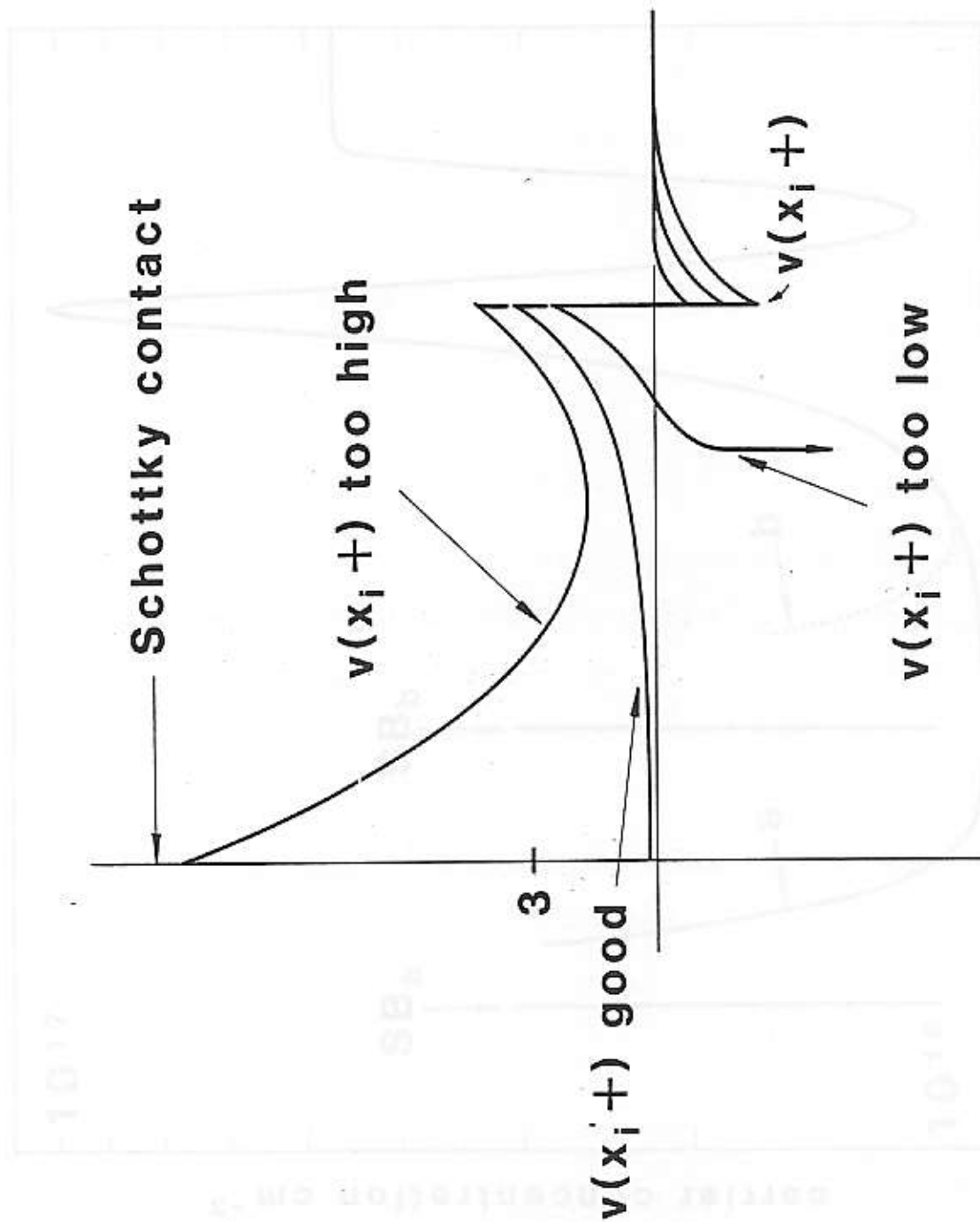


Fig. D-1 Effects of bad adjusting of the potential $v(x_i +)$.

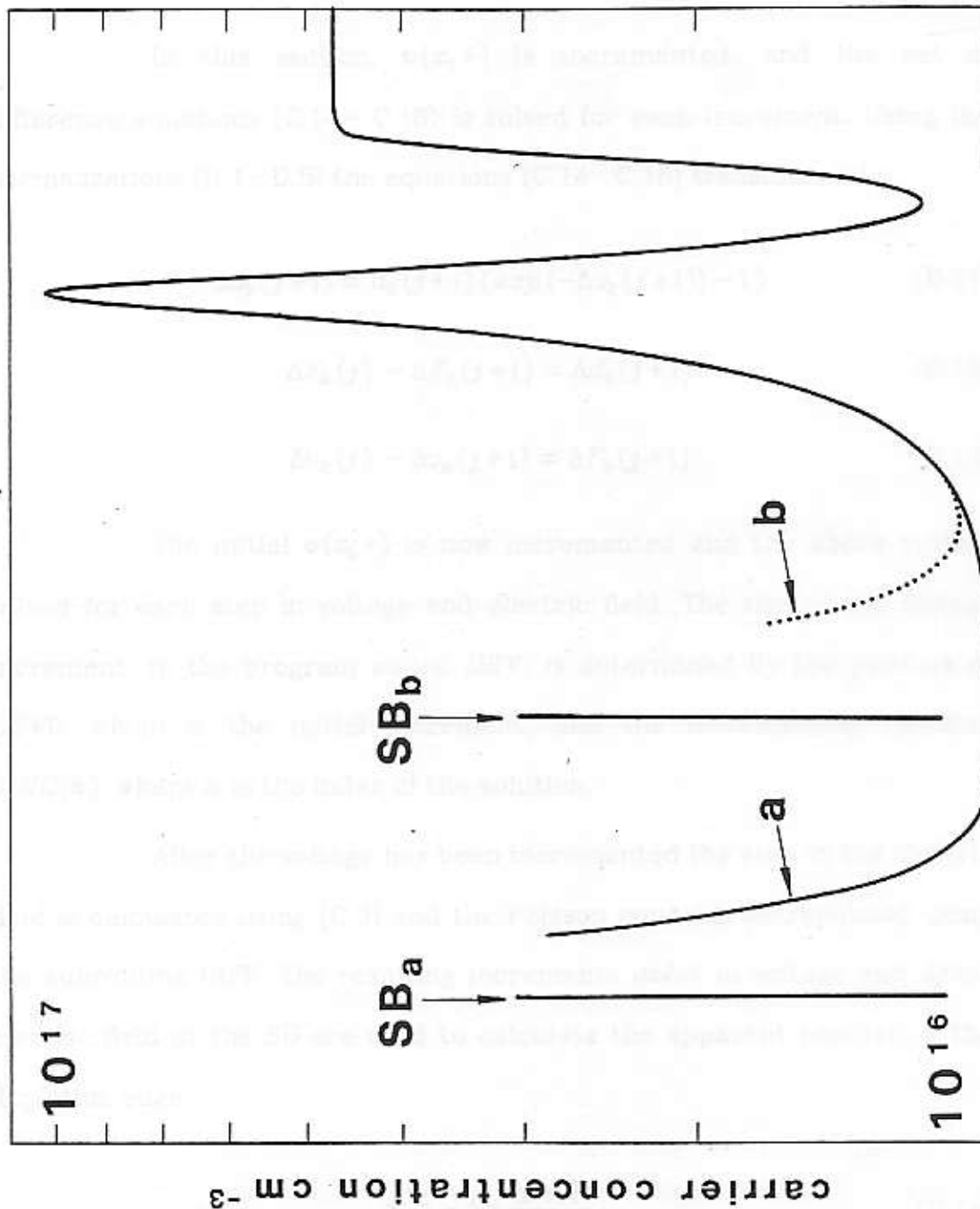


Fig. D-2

The profile (a) was obtained using the Schottky barrier SB^a which is sufficiently far away from the HJ, whereas the profile (b) is distorted because the Schottky barrier SB^b is too close.

SECTION III: Difference analysis

In this section, $v(x_i+)$ is incremented, and the set of difference equations (C.14 - C.16) is solved for each increment. Using the normalizations (D.1 - D.5) the equations (C.14 - C.16) transform into:

$$\Delta d_k(j+1) = d_k(j+1) (\exp(-\Delta v_k(j+1)) - 1) \quad (D.11)$$

$$\Delta F_k(j) - \Delta F_k(j+1) = \Delta d_k(j+1) \quad (D.12)$$

$$\Delta v_k(j) - \Delta v_k(j+1) = \Delta F_k(j+1) \quad (D.13)$$

The initial $v(x_i+)$ is now incremented and the above system solved for each step in voltage and electric field. The size of the voltage increment, in the program called *DEV*, is determined by the product of *DEV0*, which is the initial increment, and the incrementing function *VINC(k)*, where *k* is the index of the solution.

After the voltage has been incremented the step in the electric field is calculated using (C.3) and the Poisson equation extrapolated using the subroutine *DIFF*. The resulting increments *dvtot* in voltage and *dftot* electric field at the SB are used to calculate the apparent position of the depletion edge:

$$x = -\Delta x \frac{dvtot}{dftot} \quad (D.14)$$

The minus sign is used because *dftot* is negative. The carrier concentra-

tion x_n is found using,

$$x_n = \frac{dftot V_T \epsilon_1}{(x_{old} - x) q \Delta x} \quad (D.15)$$

where x_{old} is the position x from the previous solution. The pairs x_n and x are saved, they form the apparent profile. The names of variables used here correspond to those used in the program.

Checking the simulated profile

A very simple way to find out whether the profile obtained by simulation is correct is to check it by means of equations (3.3) and (3.4). If the band offset and interface charge density used in simulation are approximately equal to those obtained by integration, the simulation is well done. In the program, this is done simultaneously while the profile is being generated. When simulation is finished, the integrated ΔE and σ_i are given.

3. Appendix E: The program listing

```

C*****
C
C          SIMULATION OF C-V CARRIER CONCENTRATION PROFILING
C
C*****

      real N2,N1,Nc2,Nc1
      dimension d(2001)
      double precision DEV,v0,vx,dvtot,VHI,VLD,v,V00,R,vold,vnew,DEV00
      double precision DEF,f0,fx,dftot,fnew,fold,VMIN
      double precision x,xold,xn,xnorm1,xnorm2,A,j,D1,Ld
      double precision bk,q,eps0,e,e1,e2,sigma,sn,dec,VT,E0,Vsg
      character DMODE*1
      common /SD/ d,jmar,A
      common /S/ vx,fx,vtot,ftot,D1,dec,VT,LOG,ILOG,vmax
      common /D/ DEV,DEF,dvtot,dftot
      data bk,q,eps0 /1.38065d-23,1.60219d-19,8.85418d-14/

C..... Temperature (K)
      T=300.

C..... Type of semiconductor 1(p) or -1(n)
      TYPE=1.

C*****
C
C          HETEROJUNCTION PARAMETERS
C-----

C..... Bandgap discontinuity (eV)
      dec=0.40

C..... Interface charge density (1/cm2)
      sigma=0.40

C-----
C          Chase DMODE: 'y' or 'n' for JOYCE-DIXON correction
C-----

      DMODE='n'

C*****
C
C          SUBSTRATE PARAMETERS
C-----

C..... Doping level in the SUBSTRATE
      N2=1.e+16

C..... Effective density of states
      Nc2=4.7e+17

C..... Dielectric permittivity
      eps2=13.1

C*****
C
C          EPI-LAYER PARAMETERS
C-----

```

```

C..... maximum allowed voltage at SB
      vmax=50.
C..... Doping level in the EPI-LAYER
      N1=1. e+16
C..... Effective density of states
      Nc1=4. 7e+17
C..... Dielectric permittivity
      eps1=13. 1
C..... Thickness of the EPI-LAYER
      w=100000. *sqrt(1. eB/N1)
      w=float(ifix(w))/100000.
C..... Position step in extrapolation
      dx=w/1000.

C*****1*****
      call CHANGE(dec, sigma, N2, N1, DMODE, w, Nc2, Nc1, eps2, eps1, T, TYPE)
C*****1*****

C..... SUBSTRATE thickness
      b=. 6*w
C..... Number of discrete points in the EPI-LAYER
      jmax=w/dx
C..... Voltage equivalent of temperature
      VT=b*k*T/q

C*****1*****
C
C      NORMALIZATION
C-----

      e2=eps2*eps0
      e1=eps1*eps0

      xnorm2=(N2*2. *q*dx*dx)/(VT*e2)
      xnorm1=(q*dx*dx)/(VT*e1)

      A=xnorm1*(N2*(Nc1/Nc2))
      D1=xnorm1*N1

      EO=VT/dx
      e=eps2/eps1
      sn=(-TYPE*q*sigma)/(EO*e1)
      Ld=DSQRT(((e2*VT)/(q*N2)))
      OUTLd=SQRT(((e1*VT)/(q*N2)))

C*****1*****
C
C      MAIN PROGRAM
C-----

C*****1***** analysis of initial state *****

```



```

c----- set interval for bisection

epsmin=amin1(e2,e1)
xNmin=amin1(N2,N1)
arg=(q*sigma*sigma)/(epsmin*VT*xNmin)

c..... sigma >= 0 for N-type

if(TYPE*sigma.le.0.) Vsigma=-2.*alog(arg+1.)

c..... sigma < 0 for N-type

if(TYPE*sigma.gt.0.) Vsigma=1.+arg

Vsg=db1e(Vsigma)
Vsg=dmin1(Vsg,vmax)
VLO=DMIN1(-1.d0,Vsg,-dec/VT)
VHI=DMAX1(1.d0,Vsg,DABS(dec)/VT)

c----- head of loop

vtot=vmax
VMIN=5.d1
kkk=0
55 continue
kkk=kkk+1
if(kkk.gt.100) then
    VOO=VMIN
    go to 1001
end if

c----- boundary cond. at interface on the substrate side

VOO=(VLO+VHI)*5.d-1

c----- calculation of v0 and f0

1001 continue

if(DMODE.ne.'y') then
    f0=-sign(1.,VOO)*DSQRT(xnorm2*(VOO-1.d0+dexp(-VOO)))
    v0=VOO
    R=db1e(N2)*DEXP(-VOO)
else
    R=db1e(N2)*DEXP(-VOO)
    if (R.gt.20.1*Nc1) then
        LOG=-1
        go to 56
    endif
    call DIXON(f0,v0,R,N2,Nc2,xnorm2)
endif

c----- boundary cond. at interface on epi-layer side

```

```

fx=a*f0-sn
vx=v0+dec/VT

c----- iteration toward the surface

call STAT
if(LOG.eq.1) print*, '*'
if(LOG.eq.-1) print*, ' -'

56 continue
if(kkk.gt.100) go to 1002

c----- memorizing V00 which gives smallest Vsb,
c----- but Vsb < 3VT is not met.

if (vtot.gt.0. and. vtot.lt.vmax) VMIN=DMIN1(V00,VMIN)

c----- readjusting of boundary cond.

if (LOG.gt.0) then
  VHI=V00
  go to 55
else if (LOG.lt.0) then
  VLO=V00
  go to 55
endif

c----- checking whether vtot < vmax

1002 continue
if(vtot.ge.vmax) then
  write(6,4000)
  go to 3000
endif

c----- checking for accumulation overload

if(R.gt.Nc2.and.DMODE.eq.'n') print*, ' * ACCUMULATION OVERLOAD *',
*' Use JD approximation'
if(R.gt.20.*Nc2.and.DMODE.eq.'y') print*, ' * ACCUMULATION',
*' OVERLOAD *'

c----- printout

call pout(w,T,dec,sigma,TYPE,N2,N1,Nc2,Nc1,eps2,eps1)
write(6,4001)v0,vx
4001 format(/,' Band spike/notch in SUBSTRATE',f8.3,' in EPI-LAYER ',
*f8.3)

qrt=0.
art=1.
qacc=0.

```

```

if(v0.le.vx.and.v0.le.0.) then
    qrt=-v0*VT
    ert=f0*EO
    qacc=ert*e2/q
else if(vx.lt.v0.and.vx.le.0.) then
    qrt=-vx*VT
    ert=fx*EO
    qacc=-ert*e1/q
endif

www=3.*qrt/ert
print*, 'Depth of notch', qrt, 'V Accumulated charge', qacc, ' 1/cm2'
print*, 'Thickness of accumulation', 10000.*abs(www), 'micrometers'

106 write(6,106)Vtot
    format(/, ' Voltage at Schottky Barrier ', f6.2, ' *VT', /, /,
    * ' START DIFFERENCE ANALYSIS ', 50('-', /))

c*****ix***** difference analysis *****ix*****
c----- integration parameters

xstart=.3*w
xend=1.6*w
CHARGE=0.
DECALC=VT*log((Nc1*N2)/(Nc2*N1))
g=q/e1

c----- output file opening

open(unit=1, file='output', status='old')
close(unit=1, status='delete')
open(unit=1, file='output', status='new')
rewind 1

c----- voltage incrementing parameters

v=v0
c..... Starting increment DEVO
DEVO=1.0d-9
c..... Speeding factor kx
kx=270

c----- Calculating voltage and field

if(DMODE.ne.'y') then
    fold=-dsign(e,v)*DSGRT(xnorm2*(v-1.d0+dexp(-v)))-sn
else
    R=db1e(N2)*DEXP(-v)
    call DIXON(fold,vold,R,t2,Nc2,xnorm2)
    fold=e*fold-sn
endif

```

```

c----- voltage incrementing
do 3 k=1,3000
    rk=float(k)
    CORR=VINC(k,kx)
    DEV00=DEV0+CORR
    v=v+DEV00
    if(DMODE.ne.'y') then
        fnew=-dsign(e,v)*DSQRT(xnorm2*(v-1.d0+dexp(-v)))-sn
    DEV=DEV00
    else
        R=db1e(N2)*DEXP(-v)
        call DIXON(fnew,vnew,R,N2,Nc2,xnorm2)
        fnew=e*fnew-sn
    DEV=vnew-vold
    endif
    DEF=fnew-fold

c----- extrapolating towards S3

    call DIFF

    vtot=vtot+dvtot
    fold=fnew
    vold=vnew

c----- position calculation

    x=-dx*(dvtot/dftot)

c----- concentration calculation

    if (k.ne.1).then
        xn=(dftot*dx)/((xold-x)*xnorm1)

c----- printout

    if (x.ge.xstart) then
        yred=sngl(x*10000.)
        ynred=sngl(xn)
        write(1,107)yred,ynred
    endif

c----- integration for CHARGE and calculated DE

    if (x.gt.xstart) then
        if (x.lt.w) then
            CHARGE=CHARGE+(x-xold)*(N1-xn)*TYPE
            DECALC=DECALC+g*(xn-N1)*(x-w)*(x-xold)
        else if (x.lt.xend) then
            CHARGE=CHARGE+(x-xold)*(eps2*N2/eps1-xn)*TYPE
            DECALC=DECALC+g*(xn-eps2*N2/eps1)*(x-w)*(x-xold)
        end if
    end if
else

```



```

      vn=vj
      j=j-1
      d(j+1)=A*dexp(-vn)
      fj=fn+d(j+1)-D1
      vj=vn-fj

      if (vj.le.3.and.vj.ge.0) ILOG=1
      if (vj.gt.vg) then
        LOG=1
        go to 2
      else if (vj.lt.vl) then
        LOG=-1
        go to 2
      endif

1    continue
      vtot=vj
      ftot=fj
      if(vtot.gt.3.) LOG=1
      if(vtot.le.0.) LOG=-1
2    continue
      return
      end

```

C..... difference equation solving

```

      subroutine DIFF
      dimension d(2001)
      common /SD/ d,jmax,A
      common /D/ DEV,DEF,dvtot,dftot
      double precision DEV,DEF,dfn,dvn,dfj,dvj,dvtot,dftot,d,A,dn
      dfj=DEF
      dvj=DEV
      j=jmax
      do 1 i=1,jmax
        dfn=dfj
        dvn=dvj
        j=j-1

        dn=d(j+1)*(dexp(-dvn)-1.DO)
        d(j+1)=d(j+1)+dn
        dfj=dn+dfn
        dvj=dvn-dfj
1      continue
      dvtot=dvj
      dftot=dfj
      return
      end

```

C..... voltage incrementing

```

      function VINC(k,kx)

```

```

p=15.
rk=float(k)
rx=float(kx)
z=exp(rx/p)
a=exp(rx/p)/(rx*rx)
VINC=1.+a*z/(a+z/(rk*rx))

return
end

```

C..... Joyce-Dixon approximation

```

subroutine DIXON(F,V,RR,DD,DC,xnorm2)
double precision F,V,xnorm2,RR,DDD,DDC
double precision g,p,d,A1,A2,A3,A4,B1,B2,B3,B4

DDD=dbl(DD)
DDC=dbl(DC)

g=RR/DDC
p=DDD/DDC
d=RR/DDD

A1 = 0.35355339
A2 = -4.95009e-3
A3 = 1.48386e-4
A4 = -4.42563e-6

V = - ( dlog(d) + A1*(g-p) + A2*(g*g-p*p)
* + A3*(g**3-p**3) + A4*(g**4-p**4))

B1 = g * (1.d0 - d * .5d0) - p * 0.5d0
B2 = g*g * (1.d0 - d * .66666666) - p*p * .3333333
B3 = g**3 * (1.d0 - d * .75d0) - p**3 * .25d0
B4 = g**4 * (1.d0 - d * .80d0) - p**4 * .20d0

F = dlog(d) + 1.d0 - d + A1*B1 + A2*B2 + A3*B3 + A4*B4
F = - DSIGN(1.d0,V)*DSQRT(-xnorm2*F)

return
end

```

C..... printout

```

subroutine pout(w,T,dec,sigma,TYPE,N2,N1,Nc2,Nc1,eps2,eps1)
real N2,N1,Nc2,Nc1
character typ*1
double precision dec,sigma
if(TYPE.eq.1.) then
    typ='P'
else
    typ='N'
endif

```

```

print*, 'DATA: '
write(6, 101)
101 format(80(' '))
print*, 'Temperature: ', T, 'K   Semiconductor is ', typ, ' type'
print*, '
print*, 'Band discontinuity: ', sngl(1000.*dec), 'meV'
print*, 'Interface charge: ', sngl(sigma), '1/cm2'
print*, '
print*, 'SUBSTRATE: N2: ', N2, 'cm-3   EPI-LAYER:   N1: ', N1, 'cm-3'
print*, '                Nc2: ', Nc2, 'cm-3           Nc1: ', Nc1, 'cm-3'
print*, '                eps2: ', eps2, '           eps1: ', eps1
print*, '
print*, 'Distance from SB to HJ: ', 10000.*w, 'micrometers'
100 format(80(' '))
return
end

```

C..... changing of parameters

```

subroutine CHANGE(dec, sigma, N2, N1, DMODE, w, Nc2, Nc1, eps2, eps1, T,
*TYPE)
real N2, N1, Nc2, Nc1
character DMODE*1, TYP*1
double precision dec, sigma

q=1.60217e-19
bk=1.38066e-23

write(6, 100)
100 format(80('*'), //, 10x, ' Welcome to CV Carrier Concentration ',
*'Profiling Program', //, 80('-'), //, 13x, 'The constants for cal',
*'culation are already set', //, 13x, 'If you dont want to change ',
*'them, type "0"', //, //)

print*, 'Temperature is 300 K, type in if different.'
read*, Te
if(Te.ne.0.) T=Te
VT=bk*T/q

write(6, 110)
110 format(' The program already contains parameters for following'
*' crystals: ', //, //)
write(6, 1199)
1199 format(10x, '1 GaAs', //, 10x, '2 Al(x)Ga(1-x)As', //, 10x, '3 Ga'
*'P', //, 10x, '4 Si', //, 10x, '5 none of above', //)
write(6, 1101)
1101 format(' Chose the SUBSTRATE material: ')
read*, KTL
if(KTL.ne.2) go to 1299
write(6, 111)
111 format(' Type in the composition "x"')
read*, x
1299 write(6, 112)
112 format(' What is the type of semiconductor? n or p')

```



```

      read*, TYP
      if(TYP.eq. 'n') TYPE=-1.
      if(TYP.eq. 'p') TYPE=1.

      call DATA(Nc2, eps2, T, KTL, x, TYPE, VT)

      write(6, 113)
113  format(' Chose the EPI-LAYER material', /)
      write(6, 1199)
      read*, KTL
      if(KTL.ne. 2) go to 1298
      write(6, 111)
      read*, x
1298  continue

      call DATA(Nc1, eps1, T, KTL, x, TYPE, VT)

      write(6, 115)dec*1000.
115  format(' The bangap discontinuity going from the bulk towards'
* ' SB is: ', f7.3, ' eV')
      write(6, 102)
      read*, z
      if(z.ne. 0.) dec=z

      write(6, 101)sigma
101  format(' Interface charge density is ', 1pd9.2)
      write(6, 102)
102  format(' If you want to change, type in new value:')
      read*, z
      if(z.ne. 0.) sigma=z

      write(6, 103)
103  format(/, 80('-', /)
      write(6, 104)N2
104  format(' The doping level in the substrate is N2=', 1pe8.2)
      write(6, 102)
      read*, zz
      if(zz.ne. 0.) N2=zz

      write(6, 105)N1
105  format(' The doping level in the epitaxial layer is N1=', 1pe8.2)
      write(6, 102)
      read*, zzz
      if(zzz.ne. 0.) N1=zzz

      write(6, 106)
106  format(/, ' Do you want Joyce-Dixon correction in the SUBSTRATE?',
* '(y/n): ')
      read*, DMODE

      w=10000000000.*sqrt(1./N1)
      w=aint(w)/100000.
      write(6, 107)w*10000.
107  format(/, ' Epi-layer thickness: w=', f7.3, ' um Change: ')
      wq=w
      read*, zzzz

```

```

      if (zzzz.ne.0.) w=zzzz+1.e-4
      nnn=1000*w/wq
      print*, ' Number of mesh points:', nnn
      print*, ' Please wait, the intrinsic carrier distribution',
      *'is being generated'

      return
      end

C ----- data for some semiconductors

      subroutine DATA(EFF, EPS, T, KTL, x, TYPE, VT)
C -----
      real nG, mL, mX, mH, mE
      go to (1, 2, 3, 4, 5), KTL
C -----
1      continue
      x=0.
2      continue

C      GaAs - AlGaAs - AlAs
C      data taken from Casey and Panish: Heterostructure Lasers
C -----

      EPS=13.1-3.*x

      mG=0.067+0.063*x
      mL=0.55+0.12*x
      mX=0.85-0.07*x
      mH=0.48+0.31*x

      if (TYPE.eq.-1.) then
        if (x.le..45) eG=(1.424+1.247*x)/VT
        if (x.gt..45) eG=(1.424+1.247*x+1.147*(x-0.45)*(x-0.45))/VT
        eL=(1.708+0.642*x)/VT
        eX=(1.9+1.125*x+1.143*x*x)/VT

        if (x.le..45) then
          a=mG**1.5+mL**1.5*exp(eG-eL)+mX**1.5*exp(eG-eX)
          EFF=2.5e19*a*(T/300.)**1.5
          a=a+.66
          go to 1000
        else
          a=mG**1.5*exp(eX-eG)+mL**1.5*exp(eX-eL)+mX**1.5
          EFF=2.5e19*a*(T/300.)**1.5
          a=a+0.66
          go to 1000
        endif
      else
        a=mH
        EFF=2.5e19*(a*T/300.)**1.5
        go to 1000
      endif

```

```

c*****
3  continue

c  GaP
c  data taken from Sze: Physics of Semiconductor Devices
c-----

c  Indirect gap, 6 half valleys at the X point
mE=0.82
mH=0.60

if(TYPE.eq.-1.) a=mE
if(TYPE.eq.1.) a=mH

EFF=7.5e19*(a*T/300.)**1.5
EPS=11.1

go to 1000

c*****
4  continue

c  Si
c  data taken from Sze: Physics of Semiconductor Devices
c-----

c  Indirect gap, 6 valleys

if(TYPE.eq.-1.) a=2.8e19
if(TYPE.eq.1.) a=1.04e19

EFF=a*(T/300.)**1.5
EPS=11.9

go to 1000

c*****
5  continue

print*, 'Enter effective density of states in CM-3:'
read*, EFF
print*, 'Enter dielectric permittivity (e/e0):'
read*, EPS

c-----
1000 continue

c*****

return
end

```

15. References

- [1] H. Kroemer, " Heterostructure Bipolar Transistors and Integrated Circuits," *Proc. IEEE*, Vol. 70, No. 1, pp. 13-25, 1982.
- [2] H. Kroemer, " Heterostructure Bipolar Transistors: What should we build?," *J. Vac. Sci. Technol. B*, Vol. 1, No. 2, pp. 126-130, 1983.
- [3] T. Mimura, " The Present Status of Modulation-doped and Insulated-gate Field-effect Transistors in III-V Semiconductors," *Surf. Sci.*, Vol. 113, pp. 454-463, 1982.
- [4] D. Delagebeaudeuf and N.T. Linh, " Metal - (n)AlGaAs - GaAs Two-Dimensional Electron Gas FET," *IEEE Trans. Electron Devices*, ED-29, No. 1, pp. 955-960, 1982.
- [5] H.C. Casey and M.B. Panish, " Heterostructure Lasers," New York, Academic Press, 1978.
- [6] H. Kressel and J.K. Butler, " Semiconductor Lasers and Heterojunction LEDs," New York, Academic Press, 1977.
- [7] R.L. Anderson, " Experiments on Ge-GaAs Heterojunctions ", *Solid State Electron.*, Vol. 5, pp. 341-351, 1962.
- [8] W.R. Frensley and H. Kroemer, " Theory of the energy-band lineup at an abrupt semiconductor heterojunction," *Phys. Rev. B* Vol. 16, No. 6, pp. 2642-2652, 1977.

- [9] W.A. Harrison, "Elementary theory of heterojunctions," *J. Vac. Sci. Technol.*, Vol. 14, No. 4, pp. 1016-1021, 1977.
- [10] E.A. Kraut, R.W. Grant, J.R. Waldrop, and S.P. Kowalczyk, "Precise Determination of the Valence-Band Edge in X-Ray Photoemission Spectra: Application to Measurement of Semiconductor Interface Potentials," *Phys. Rev. Lett.*, Vol. 44, No. 24, pp. 1620-1623, 1980.
- [11] S.P. Kowalczyk, E.A. Kraut, J.R. Waldrop, and R.W. Grant, "Measurement of ZnSe-GaAs(110) and ZnSe-Ge(110) heterojunction band discontinuities by x-ray photoelectron spectroscopy (XPS)," *J. Vac. Sci. Technol.*, Vol. 21, No. 2, pp. 482-485, 1982.
- [12] R. Dingle, *Festkörperprobleme / Advances in Solid State Physics*, ed. by H.J. Queisser (Vieweg, Braunschweig, 1975), Vol. 15, p. 21.
- [13] H. Kroemer, "Heterostructure devices: A device physicist looks at interfaces," *Surf. Sci.* Vol. 132, pp. 543-576, 1983.
- [14] E.S. Yang, "Fundamentals of semiconductor devices," McGraw-Hill, 1978, sections 4-3, 4-10, and 5-1.
- [15] C. Kittel and H. Kroemer, "Thermal physics," W.H. Freeman and Company, San Francisco, Second Edition, 1980, pp. 373-378.
- [16] J.L. Shay and S. Wagner, "Heterojunction band discontinuities," *Appl. Phys. Lett.*, Vol. 28, No. 1, pp. 31-33, 1976.
- [17] H. Kroemer, Wu-Yi Chien, J.S. Harris, and D.D. Edwall, "Measurement of isotype heterojunction barriers by C-V profiling," *Appl.*

- Phys. Lett.*, Vol. 36, No. 4, pp. 295-297, 1980.
- [18] R. People, K.W. Wecht, K. Alavi, and A.Y. Cho, "Measurement of the conduction-band discontinuity of molecular beam epitaxy grown $In_{.52}Al_{.48}As / In_{.53}Ga_{.47}As$, $N-n$ heterojunction by C-V profiling," *Appl. Phys. Lett.* Vol. 43, No. 1, pp. 118-120, 1983.
 - [19] M.O. Watanabe, J. Yoshida, M. Mashita, T. Nakanisi, and A. Hojo, "C-V profiling studies on MBE-Grown GaAs/AlGaAs heterojunction interface," Extended Abstracts of the 16th (1984 International) Conference on Solid State Devices and Materials, Kobe, pp. 181-184, 1984.
 - [20] M. Ogura, M. Mizuta, K. Onaka, and H. Kukimoto, "A capacitance investigation of InGaAs/InP isotype heterojunction," *Jap. J. Appl. Phys.*, Vol. 22, No. 10, pp. 1502-1509, 1983.
 - [21] H. Kroemer and Wu-Yi Chien, "On the theory of Debye length averaging in the C-V profiling of semiconductors," *Solid State Electron.*, Vol. 24, pp. 655-660, 1981.
 - [22] W.C. Johnson and P.T. Panousis, "The influence of Debye length on the C-V measurement of doping profiles," *IEEE Tran. Electron Devices*, Vol. ED-18, No. 10, pp. 965-973, 1980.
 - [23] M. Nishida, "Depletion approximation analysis of the differential capacitance-voltage characteristics of an MOS structure with non-uniformly doped semiconductors," *IEEE Trans. Electron Dev.*, Vol.

- ED-26, No. 7, pp. 1081-1085, 1979.
- [24] R.C. Miller, W.T. Tsang, and O. Munteanu, " Extrinsic layer at $Al_xGa_{1-x}As / GaAs$ interfaces," *Appl. Phys. Lett.*, Vol. 41, No. 4, pp. 374-376, 1982.
 - [25] Y. Zohta, " Frequency dependence of C and $\Delta V / \Delta(C^{-2})$ of Schottky barriers containing deep impurities," *Solid-State Electron.*, Vol. 16, pp. 1029-1035, 1973.
 - [26] H. Kroemer, unpublished derivation incorporating the interface charge into the intercept method.
 - [27] Wu-Yi Chien, " The C-V and I-V characteristics of GaAs-(AlGa)As n-N heterojunctions," Ph.D. dissertation, University of California, Santa Barbara, June 1981.
 - [28] H. Kroemer, " Analytic approximations for degenerate accumulation layers in semiconductors, with applications to barrier lowering in isotype heterojunctions," *J. Appl. Phys.*, Vol. 52, No. 2, pp. 873-878, 1981.